

Beamforming in LTE FDD for Multiple Antenna Systems

ATEF HATAHET

ANKIT JAIN

MASTER'S THESIS

DEPARTMENT OF ELECTRICAL AND INFORMATION TECHNOLOGY

FACULTY OF ENGINEERING | LTH | LUND UNIVERSITY



Beamforming in LTE FDD for Multiple Antenna Systems

Master's Thesis

By

Atef Hatahet (at7232ha-s@student.lu.se)

Ankit Jain (an3783ja-s@student.lu.se)

Department of Electrical and Information
Technology
Lund University

May-2018



LUND UNIVERSITY

Abstract

High data rate is still the most crucial factor in cellular systems, and with 5g approaching new techniques are studied to achieve higher bit rates. Using MIMO technology, the spatial domain was exploited through beamforming and multiplexing multiple users' data together assured more spectrum efficiency which resulted in higher bit rates. Reciprocity based beamforming is feasible in TDD systems due to channel reciprocity assumption between uplink and downlink, the same is not true for FDD systems, as a consequence of using different frequencies between uplink and downlink. Nonetheless, FDD systems are widely deployed because of the existing spectrum assignments and earlier technologies. In addition, FDD systems have advantages such as greater coverage, lower latency over TDD systems

The thesis objective is to study the feasibility of applying beamforming in FDD systems. We investigate for appropriate techniques based on uplink channel measurements and study its performance for various conditions like Doppler shift, number of users, and also compare those results with beamforming in TDD. Results are generated by implementing LTE physical layer and a practical channel model in MATLAB. Mainly three techniques are implemented, all of these used reciprocity in term of Angle of Arrival between uplink and downlink for an FDD channel.

The obtained results showed that channel reciprocity based TDD systems perform much better than channel non reciprocity based FDD system in terms of number of users which can be beamformed with an acceptable Bit Error Rate (BER). Also, the used beamforming techniques showed around 50% improvement in overall capacity for one cell, when compared to FDD system with no beamforming applied.

Acknowledgement

We would like to thank Lars Thorsson for giving us the opportunity to work on this master thesis at Ericsson, and a special thanks to Harish Venkatraman Bhat for his supervision over all the thesis period and his dedication to make this thesis work. We also would like to express our gratitude to Fredrik Tufvesson for his valuable feedback and guidance.

This thesis has been done during our scholarship period thanks to a Swedish Institute scholarship.

At last, we could not have reached this point without the support from our families and friends.

Preface

This thesis work was done at Ericsson in Lund, for approximately 5 months. Both authors were actively involved in all the thesis work. Different methods were searched separately, however, it was discussed thoroughly and implemented together, and most importantly, coffee breaks were also taken together, where most of the discussion happened.

Contents

1	Introduction	1
1.1	Background and motivation	1
1.2	Purpose and aims	2
1.3	Methodology	2
1.4	Limitation	3
1.5	Authors contribution	3
2	Technical background	4
2.1	OFDMA and SC-OFDMA	4
2.2	LTE resource grid	5
2.3	Data transmission in LTE	8
2.4	Data reception in LTE	10
2.5	Reference signals	11
2.6	MIMO systems	11
2.6.1	Single-user (SU) multi-user (MU) MIMO	11
3	Wireless channel models	13
3.1	Introduction	13
3.2	Different channel models	13
3.3	WINNER2 channel	14
3.3.1	Channel parameters generation	15
3.3.2	Propagation scenarios	17
3.3.3	FDD modeling	17
3.3.4	Path loss model	18
3.3.5	Shadow fading	18
3.3.6	Ricean factor	18
3.3.7	Coherence time	18
3.3.8	Coherence bandwidth	19
3.4	Noise	19
3.5	Uplink and downlink channel representation	20
4	Beamforming	23
4.1	Introduction	23
4.2	Beamforming techniques	24
4.2.1	Matched filtering (MF)	24
4.2.2	Zero forcing (ZF)	24
4.2.3	Regularized zero forcing (RZF)	25
4.3	Beamforming in LTE	25
4.4	Beamforming in time division duplex systems	26
4.5	Beamforming in frequency division duplex systems	26
4.5.1	Matched array	27
4.5.2	Directional based transformation	27
4.5.3	Covariance matrix transformation	28
4.6	Joint user grouping and beamforming	33

5	System model using MATLAB	34
5.1	Initial parameters	34
5.2	Uplink	34
5.3	Downlink	37
6	Results	39
6.1	SINR and number of users	39
6.2	BER and number of users	42
6.3	Performance with number of antennas	44
6.4	Performance with Doppler shift	45
6.5	Computational complexity	46
6.6	Performance limitation	46
7	Conclusions and future work	49

List of Figures

1	Spectral efficiency comparison between multicarrier modulation (a) and OFDM (b).	5
2	OFDM transmitter, inspired from [15].	6
3	LTE time domain structure, inspired from [17].	7
4	LTE Resource grid structure.	7
5	Constellation diagram for the modulation schemes used.	9
6	Data transmission block diagram.	10
7	Data Reception block diagram.	10
8	Comparison between SU-MIMO and MU-MIMO.	11
9	Geometric based channel model representation, source: [31].	15
10	The effect of Doppler spread on the channel frequency transfer function at center frequency.	19
11	TDD for short duplex time.	26
12	TDD for long duplex time.	27
13	FDD for long duplex time.	27
14	Capon spatial covariance transformation steps, source [12].	29
15	APS Modification by the weighting window (dotted black), red part will be used to calculate covariance matrix, the rest is assumed to be interference.	30
16	GUI of the MATLAB model.	35
17	Probability of $\text{SINR} \geq 3$ dB vs number of users for D1 LOS scenario.	40
18	Probability of $\text{SINR} \geq 3$ dB vs number of users for D1 NLOS scenario.	40
19	Probability of $\text{SINR} \geq 3$ dB vs number of users for B1 LOS scenario.	41
20	Probability of $\text{SINR} \geq 3$ dB vs number of users for B1 NLOS scenario.	41
21	Average BER vs number of users for D1 LOS scenario.	42
22	Average BER vs number of users for D1 NLOS scenario.	42
23	Average BER vs number of users for B1 LOS scenario.	43
24	Average BER vs number of users for B1 NLOS scenario.	43
25	Probability of $\text{SINR} \geq 3$ dB vs number of BS antennas for B1 NLOS scenario.	44
26	Probability of $\text{SINR} \geq 3$ dB vs Doppler shift for B1 NLOS scenario.	45
27	AOA-ZF group beamforming performance.	47
28	FC group beamforming performance.	48

LIST of ABBREVIATIONS

AOA - Angle of Arrival
AOD - Angle of Departure
APS - Angular Power Spectrum
BER - Bit Error Rate
BS - Base Station
BW - Bandwidth
CP - Cyclic Prefix
CRC - Cyclic Redundancy Check
CSI - Channel State Information
DCCM - Downlink Covariance Channel Matrix
DL-SCH - Downlink Physical Shared Channel
DM-RS - Demodulation Reference Signal
FC - Frequency Calibration
FDD - Frequency Division Duplex
GSCM - Geometry Based Stochastic Channel Model
IMT - International Mobile Telecommunications
IO - Intermediate Object
ISI - Inter Symbol Interference
LOS - Line-of-Sight
LTE - Long Term Evolution
MIMO - Multiple Input Multiple Output
MMSE - Minimum Mean Squared Error
MPC - Multi Path Component
MRT - Maximum Ratio Transmission
MU-MIMO - Multi User MIMO
MUSIC - Multiple Signal Classification
NLOS - Non Line-of-Sight
OFDMA - Orthogonal Frequency Division Multiple Access
OFDM - Orthogonal Frequency Division Multiplex
PDF - Probability Density Function
RZF - Regularize Zero Forcing
SC-OFDM - Single Carrier Orthogonal Frequency Division Modulation
SINR - Signal to Interference Plus Noise Ratio
SNR - Signal to Noise Ratio
SRS - Sounding Reference Signal
SU-MIMO - Single User MIMO
TDD - Time Division Duplex
TB - Transport Block
TTI - Transmission Time Interval
UCCM - Uplink Covariance Channel Matrix
UE - User Equipment
UP-SCH - Uplink Physical Shared Channel
WINNER - Wireless World Initiative New Radio
ZF - Zero Forcing

1 Introduction

With the evolution of the GSM system throughout the 1980s, telecommunication services became economically cheaper and thus became available to mass population. First, telecommunication services were mostly concentrated around voice and short messages service. Then, with the integration of Internet with telecommunication services, there is a sudden surge for demand of high data rate, nonetheless, spectral efficiency has always been the bottle neck for high data rate. Thanks to Long Term Evolution (LTE), orthogonal frequency division multiplex (OFDM) technique and multiple antennas systems, high data services like HD video streaming, live gaming and on-line TV is now available to mass population to affordable prices. Now, it became a hot topic not only to connect people but also devices and vehicles with cellular systems. It became quite clear that desire for high data rates will never end.

Multiple antennas systems have the potential to be the key technique for achieving high capacity and reliable transmission in wireless communication systems. High capacity can be achieved by spatial multiplexing, while reliability can be achieved by diversity transmission [1]. Hence, Multiple antennas systems (MIMO) is the key technique in LTE, and Massive MIMO will play a crucial role in 5G [2].

In wireless cellular based systems, interference is one of the major limiting factors to achieving high capacity, as a possible solution, beamforming can be used, which is a technique that uses space signal processing in order to adjust the weights in the antenna array to direct the energy in a certain direction, in presence of noise and interference. This could provide higher throughput at the user end and thus, better spectral efficiency [3].

1.1 Background and motivation

Beamforming in Time Division Duplex (TDD) with many antennas is more appealing than in Frequency Division Duplex (FDD) due to channel reciprocity assumption between uplink and downlink, assuming uplink and downlink occurs during the same coherence time. This will result in reasonable overhead, that is proportional only to the number of terminals served, and not related to Base Station (BS) antennas [4]. On the other hand, there are wireless communication systems which use FDD since it is more effective for symmetric traffic and delay sensitive applications, like online gaming, than TDD based systems. However, the frequency gap between uplink and downlink in FDD is large enough to eliminate the channel reciprocity assumption. As a consequence, using a huge number of BS antennas in FDD systems is somehow inefficient, as this will require overhead that would drain the whole available capacity [5]. Other techniques must be studied and tested in order to use beamforming in massive MIMO for FDD systems.

1.2 Purpose and aims

The aim of the thesis is to study and implement beamforming for MIMO-FDD LTE systems. Broadly there are two methods to estimate Channel State Information (CSI), open loop and closed loop. In closed loop, the BS estimates downlink CSI through feedback sent from the user equipment (UE), while in open loop, the BS doesn't receive any feedback from UE, thus, saves extra overhead for CSI estimation. Although there are some methods which can reduce the length of pilot signals for CSI estimation, but as the number of transmitting antennas and UEs served by each BS increases, length of the pilot signal increases exponentially. Therefore, closed loop CSI tends to become impractical for massive MIMO and high number of UEs.

As already mentioned, we cannot rely neither on channel reciprocity for FDD nor on feedback from the UE for downlink CSI, so we need to consider other parameters which remains constant for uplink and downlink, like Angle of arrival (AOA), channel spatial covariance matrix, delay and mean power of multiple path components (MPCs) [6].

There are mainly two parameters, AOA and channel covariance matrix, which are studied in details in the literature. So, the thesis work is broadly divided into 3 steps:

1. To compare angle of arrival and channel covariance matrix methods for downlink beamforming.
2. Simulate the above beamforming algorithms in LTE system using MATLAB.
3. Compare results from both methods, and with TDD system.

The purpose is to get an answer to whether it is possible to do open loop beamforming with partial downlink channel information in FDD with MIMO, and if yes, how does the performance compare to channel reciprocity based TDD solution.

1.3 Methodology

This thesis is continuation of work of masters thesis entitled 'Adaptive beamforming for Next Generation Cellular System' by S. Andersson and W. Tidelund [7]. Their aim was to implement and investigate beamforming for MIMO-TDD LTE systems. We have used their MATLAB code as a base for LTE simulation and updated it for FDD systems. Also since we need a wireless channel to model directional based information, so we updated the fading channel implemented by them with WINNER2 channel model. Once the initial setup is set, we investigated different methods for obtaining downlink CSI from uplink CSI. As per scope of thesis, we primarily concentrated on open loop, angular based transformation and channel covariance matrix based transformation methods.

We have studied and implemented these methods and compared them along with beamforming for TDD system. Comparison is based on Signal-to-Interference-plus-noise ratio (SINR), computational power and how they perform in different environments and with different number of BS antennas.

1.4 Limitation

The thesis focused on one BS with multiple UEs, so inter-cellular interference was not considered. All UEs are equipped with one antenna and have equal received power, plus, multilayer transmission will not be implemented to simplify the model. All UEs are assumed to have established a connection in advance and therefore, only data and pilot symbols will be transmitted. The BS will only use the information in the demodulation reference signals (DM-RS) not the sounding reference signal (SRS) for acquiring the uplink CSI. All our simulations are based on 3 MHz bandwidth channel as we considered almost a frequency flat channel.

1.5 Authors contribution

In this thesis work, we have successfully investigated the feasibility of implementing the work done in [4], [12], and [13] in an LTE FDD system using MATLAB simulation. However, the conclusion stated in [12] that the used method outperforms the AOA based methods does not agree with our simulation results, this is probably due to the different used channel and therefore different angular separation. In addition, beamform grouping was also investigated and successfully implemented, that is to separate different users in different groups to improve the SINR results. Also, we further investigated the SINR performance in terms of angular separation between users for [4] and the correlation between covariance matrices of users for [13].

2 Technical background

There has been a great amount of research going on for Multi User MIMO (MU-MIMO). In [3], an overview and potential of massive MIMO is given. While [8] gives the limitation of acquiring full downlink CSI using feedback, but wide area of research has been done in acquiring downlink CSI using uplink CSI. Work done in [9], [10] shows that for wireless communication with different carrier frequencies for uplink and downlink, the angle of arrival (AOA) is a constant parameter. In [11], [4] they try to directly calculate angle of arrival (AOA) for each user to estimate downlink CSI. While in [12], [13] they try to estimate downlink covariance matrix based on uplink covariance matrix under assumption of same Angular Power Spectrum (APS) in uplink and downlink.

In this section, some basic concepts of the 4th generation of mobile communications system, also known as the LTE, will be explained. Only the fundamental parts and the specifications that are used in this thesis will be discussed, as LTE is a very complex and vast system. Details about LTE can be found in [14].

To start, the definition of uplink and downlink must be stated, the first, is used for the communication link from the UE to the BS, while the latter is the opposite, from the BS to the UE.

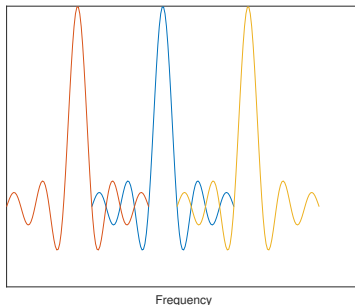
2.1 OFDMA and SC-OFDMA

Modulation and multiple access techniques have always been essential blocks in any wireless communication system for achieving a better data rate and supporting multiple users, and the orthogonal frequency division multiplexing access (OFDMA) is the cornerstone for LTE. It basically divides the frequency-selective wide bandwidth, into non frequency-selective narrow bands, which are combined together in an overlapping but orthogonal fashion using IFFT as shown in figure 1, this will obviate the use of guard bands, which yields to higher spectrum efficiency [15].

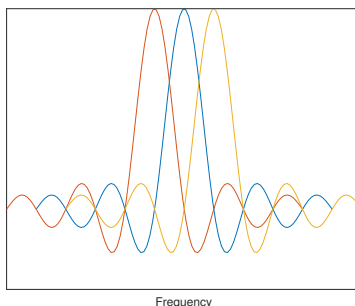
In addition, Inter-Symbol-Interference (ISI) is greatly reduced in OFDM, this can be seen as one high rate symbol stream being converted into multiple parallel orthogonal low rate streams, each with symbol period longer than the channel delay spread, which reduces ISI significantly.

Another crucial factor in the strong ability for OFDM to reduce ISI is the Cyclic Prefix (CP). As shown in figure 2, in a typical OFDM transmitter, the cyclic prefix is some kind of guard period added to the start of each OFDM symbol to eliminate the ISI caused by multipath propagation. So, the prefix is just the copy of the last m output of the IFFT at the beginning, m is chosen such that the CP length is longer than the longest channel delay. LTE defines two types of cyclic prefix, normal and extended. Normal CP will be used throughout the thesis work and will be referred to as cyclic prefix only.

It is worth mentioning that, in an OFDM system, each sub-carrier (SC) can hold different modulation schemes, as a consequence of frequency-selective channel, different sub-carriers can experience different transfer functions, therefore,



(a) multicarrier modulation



(b) OFDM

Figure 1: Spectral efficiency comparison between multicarrier modulation (a) and OFDM (b).

different modulation schemes could be used within each sub-carrier [15]. However, in this thesis work, the same modulation scheme is used in all sub-carriers.

2.2 LTE resource grid

The sub-carrier spacing for the OFDM in the LTE is $\Delta f = 15\text{kHz}$ for both uplink and downlink. Therefore, the LTE system based on FFT transmitter and receiver will have a sampling rate of $f_s = \Delta f \times N_{FFT}$ where N_{FFT} is the FFT size.

Meanwhile, in the time domain, the transmission is divided into frames, each with a length of 10 ms which is further divided into 10 subframes each with a 1 ms duration. The subframe is composed of two slots each with a length of 0.5 ms. Each slot contains 7 OFDM symbols including the cyclic prefix. Figure 3 represents a better understanding of the description above.

Now, the combination of one sub-carrier and one OFDM symbol is the smallest physical resource in the LTE system, and it is called resource element. while, the resource blocks (RBs) are a group of resource elements, where each block

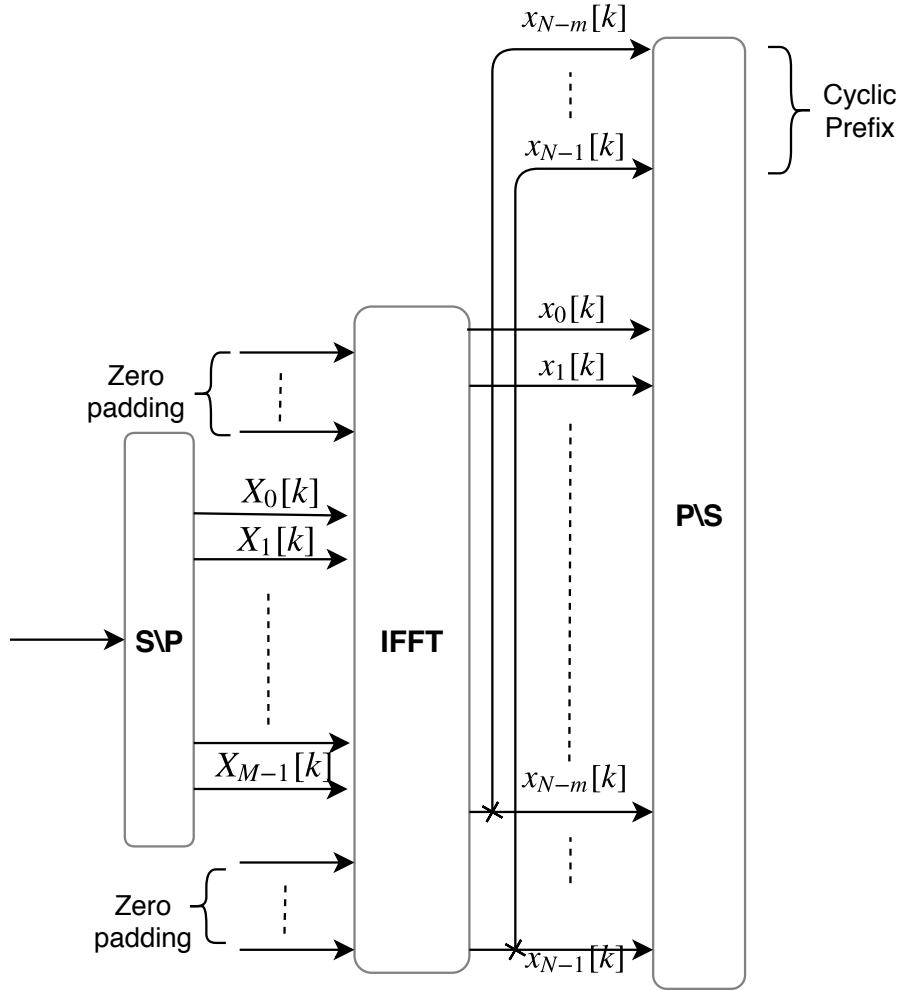


Figure 2: OFDM transmitter, inspired from [15].

contains 12 consecutive sub-carriers in the frequency domain and 1 slot in the time domain. Thus, every resource block contains $7 \times 12 = 84$ resource elements. Figure 4 shows the composition of one resource block. The total number of resource blocks available in the LTE systems depends on the number of sub-carriers, and obviously, this is related to the bandwidth used in the system. However, not all bandwidth is used for transmission, there are guards that are left in the upper and lower edges of the bandwidth [16], table 1 gives an example of resource blocks and bandwidth configuration [17].

One drawback for OFDM is that the power of its signal is subject to high variations and that yields to high power consumption. Therefore, the Single

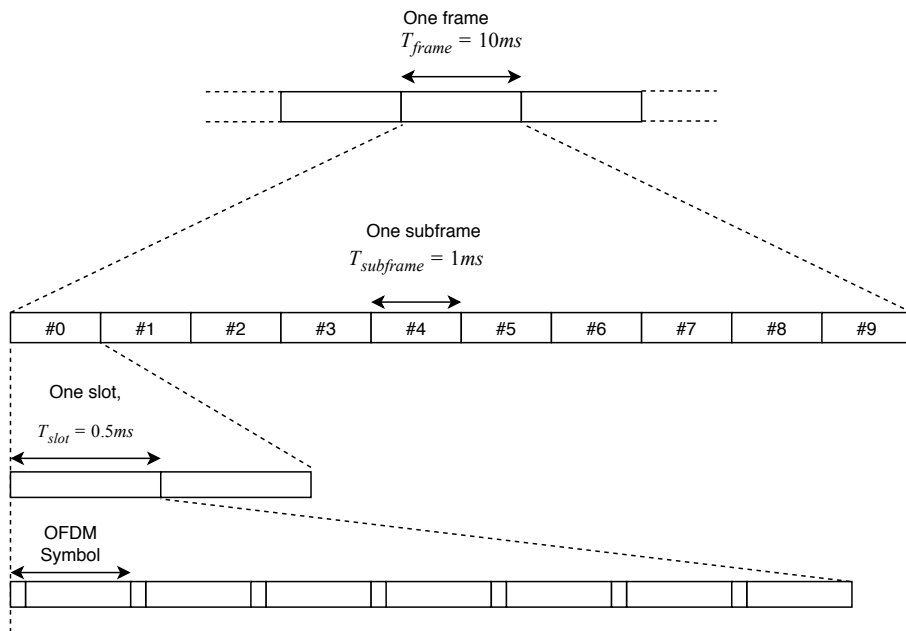


Figure 3: LTE time domain structure, inspired from [17].

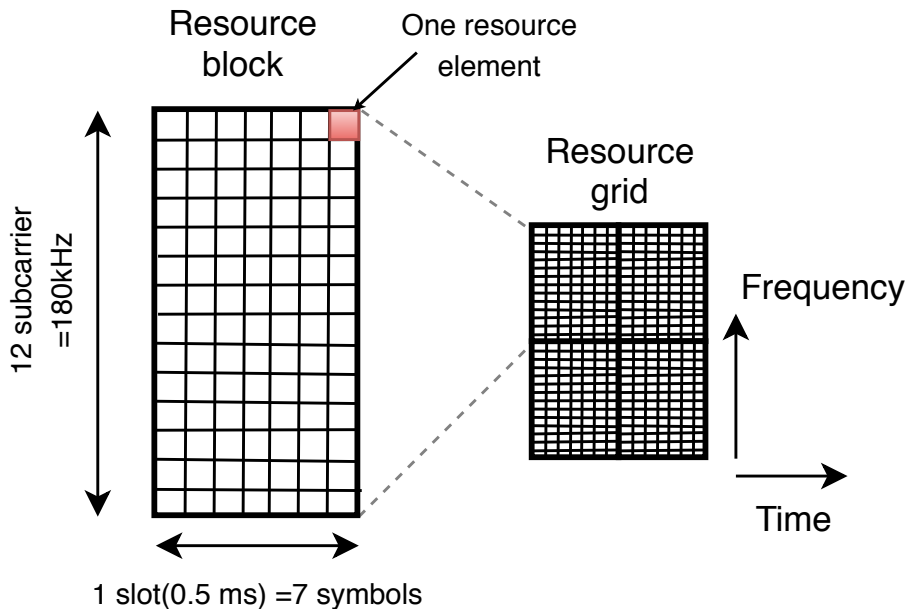


Figure 4: LTE Resource grid structure.

carrier frequency division multiple access (SC-FDMA) is used instead of the OFDMA, in the UE side where expensive power amplifier that is close to linear could not be used. The SC-FDMA mixes the symbols together before being placed on the subcarriers, unlike the OFDMA where direct symbol to subcarriers mapping is done, and the mixing between symbols that is used is another FFT [16].

Total BW (MHz)	Number of RBs	Number of SC	Occupied BW (MHz)
1.4	6	72	1.08
3	15	180	2.7
5	25	300	4.5
10	50	600	9
20	100	1200	18

Table 1: Resource blocks and BW example configurations.

2.3 Data transmission in LTE

This section describes the transmission procedure for both uplink and downlink in LTE system. In this thesis work, the UEs and the BS are considered to have already established a connection, synchronization and power control. It should be stated that in the LTE specification, there are transmission modes that correspond to different multi antenna transmission schemes, in this work, transmission mode 7 will be used and that is, non-codebook-based precoding supporting single-layer transmission [17].

In order for the data to be transported across the links, there are multiple channels that separate different types of data, we will only consider the downlink and uplink physical shared channels denoted as (DL-SCH) and (UL-SCH) respectively, they are the data-bearing channels in the LTE [15]. Data units that are transmitted on the mentioned channels are called Transport Blocks (TBs) during a time called Transmission Time Interval (TTI), which corresponds to one subframe. Depending on the multiple antennas transmission scheme used, a maximum of two TBs could be transmitted within a TTI. The data transmission is described as the steps below:

1. The transmission process starts with bit level processing like cyclic redundancy check (CRC), segmentation, coding, rate matching and scrambling shown as one block in figure 6 named bit level processing, details about mentioned processing can be found in [17].
2. Modulation is performed, where bits are transformed into complex symbols depending on the modulation scheme used. In this thesis, 3 types of schemes were used, QPSK, 16 QAM, 64 QAM shown in figure 5. Higher modulation corresponds to more bits in one symbol which yields higher bit rates. However, the BER will also increase, because of signal constella-

tions become closer to each other which results that the receiver will have higher probability in making an erroneous decision [18].

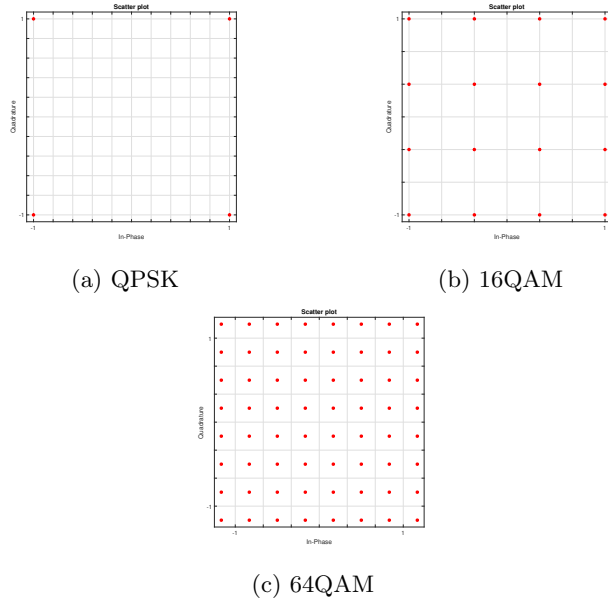


Figure 5: Constellation diagram for the modulation schemes used.

3. Resource Block mapping is performed, that is to take the symbols and assign a corresponding resource element in the available LTE resource grid, distributing the resources among the users (scheduling), is usually done at a higher layer. In this thesis, scheduling will only be considered as a fair distribution of resource blocks among users, in the case where the remainder of number of available resource block and users is not zero, the remaining resource blocks will be allocated to the last user. This is the case in uplink. While, in downlink, all users will share the same resources.
4. Precoding is performed, also known as digital beamforming, which is the topic of this thesis. Precoding is basically multiplying symbols that will be transmitted by some weights, that is calculated in a fashion to fulfill a certain requirement, more details will be discussed in section 4.
5. Precoding result is mapped to the physical antennas. Thus, every antenna will have its own weighted resource grid. In this thesis work, the beamforming is applied only in downlink side, so Precoding in uplink is not performed.
6. OFDMA and SC-FDMA modulation take place for downlink and uplink respectively, where the resource grids are transformed into waveforms as mentioned in section 2.1.

- Waveforms are being upconverted to the carrier frequency to end the transmission process.

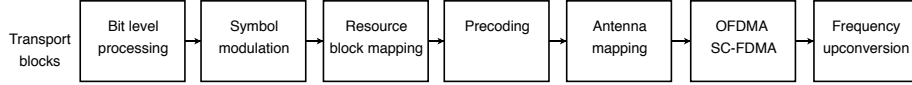


Figure 6: Data transmission block diagram.

2.4 Data reception in LTE

After the transmitted signal passes through the wireless channel, which will be discussed later, the received signal follows some kind of reverse order for what it has encountered in the transmission process, as shown in figure 7.

- The received wave is down-converted to baseband.
- OFDMA, SC-FDMA demodulation is performed for downlink and uplink respectively.
- Due to the channel effect, the transmitted signal is distorted because of fading, pathloss and other factors that will be discussed in section 3. However, the receiver should estimate the channel to compensate for the channel effect and retrieve the information, this is done with the help of the pilot signals, which are placed in specific locations in the resource grid in a way that ensures no interference between the pilot signals. Next, using their known locations and values the channel impulse response will be estimated using the least squares as described in [19]. Then, the estimates are averaged to reduce the noise effect, and then interpolation is done to estimate the entire channel response for the resource grid.
- Using the estimated channel obtained by the receiver, the channel effect is compensated using what is called channel equalization, to obtain the transmitted signal without channel distortion. Two of the most know methods of channel equalization are zero forcing (ZF) and minimum mean squared error (MMSE), the first suffers from noise enhancement, while the second is a trade-off between ISI suppression and noise enhancement [20].
- The reception process ends with symbol demodulation to retrieve the original transmitted bits.

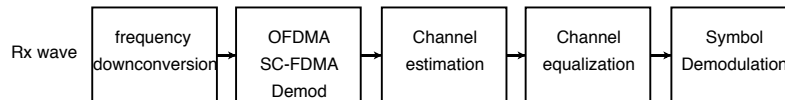


Figure 7: Data Reception block diagram.

2.5 Reference signals

Reference signals are symbols that reserve specific locations in the resource grid, to serve a certain purpose. There are multiple reference signals, however, in this work only DM-RS will be discussed.

DM-RS are used for channel estimation either by a single terminal in the downlink, when it is transmitted in the resource blocks assigned to that terminal in order for the UE to be able to estimate the channel for receiving DL-SCH, or by a base station in the uplink, also for channel estimation to perform demodulation of UL-SCH. The interference between two consecutive reference symbols is handled by using orthogonal cover codes [17].

2.6 MIMO systems

MIMO systems, refers to systems that uses multiple antennas at the transmitter and the receiver side, the use of multi antennas will activate the ability to use many signal processing techniques which lead to performance improvement. The improvement can be divided in two categories, spatial diversity and spatial multiplexing, the first refers to the case where multipath scattering is being combated, while the later exploit the multipath scattering [21].

2.6.1 Single-user (SU) multi-user (MU) MIMO

In MIMO technology, two terms must be differentiated, Single-user and Multi-user MIMO. The first can be used for conventional MIMO case, where we have one BS and one UE as shown in figure 8a, While the later is used to describe the scenario with several cellular users, and the base station performs some kind of processing, so that it can transmit using same the bandwidth and time resources, while users can differentiate their streams from each other, as depicted in figure 8b. [21]. Therefore the terminal antennas in the SU-MIMO can cooperate

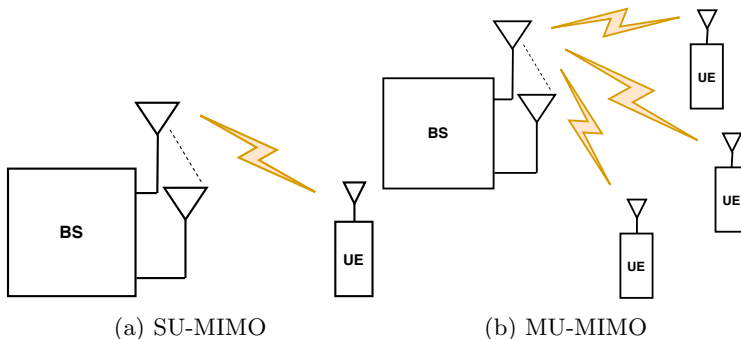


Figure 8: Comparison between SU-MIMO and MU-MIMO.

together, that is, the user can estimate the channel response over all its antennas, consequently, any type of precoding (will be discussed later) performed by the

base station that relies on the whole channel estimation, can be decoded by the UE. However the opposite is not true, as in the MU-MIMO only the BS can estimate the channel of all users, while at the receiver end, individual users can only estimate the channel experienced by their received streams and not other users channel.

In addition, the SU-MIMO has more diversity assuming that the total number of received antennas is fixed, since all the links between the base station and the received antennas corresponds to the same user, meanwhile the links in MU-MIMO belongs to multiple users. Nonetheless, the main advantage of MU-MIMO is spectral efficiency, since the same frequency channel is used for multiple users, and with the increased demand for spectrum in the interference limited systems, spectral efficiency is a crucial criteria for evaluating communication systems [1].

3 Wireless channel models

3.1 Introduction

Wireless systems performance highly depends on the wireless channel. As any transmitted signal will encounter many physical phenomena depending on the environment where the transmission process happens, which affect the amplitude and the phase of the transmitted signal. Therefore, to study and simulate wireless systems, propagation channel models are needed. Channel models are the mathematical description of different wireless propagation phenomena [6]. However, channel modelling is a very huge domain in wireless communications. So, in this section, only topics that are related to this thesis scope will be discussed.

3.2 Different channel models

A common assumption for MIMO channels is that channel matrix consist of independently and identically distributed complex Gaussian gains. But this assumption mostly leads to better results in terms of capacity. However, in practice and due to correlation between transmitting and receiving antennas' elements and LOS components, the validity of uncorrelated channel no more holds.

One widely used channel model called the Kronecker model assumes that spatial correlation between transmitting and receiving antennas are separable [22]. However, in reality spatial correlation matrix of transmitter and receiver are not completely independent [23]. The Weichselberger model attempts to overcome the Kronecker model assumption by introducing coupling between the links. But, both above mentioned models are analytical based model and doesn't completely reflect the geometrical properties of the channel. Another drawback is that they don't capture time varying properties of the channel [24].

Another widely used channel models fall under class of geometry based stochastic channel models (GSCM) [25]. In this approach the location of intermediate objects (IOs) are defined according to the probability density function (PDF) of their position, then, components of MPCs can be obtained by ray tracing on these IO. MPCs which falls under same IO constitute a cluster. In general, GMSC based model have the following advantages [26]:

1. Time varying property of channel can be captured by the movement of cluster.
2. The position of IO reflects the directional property of the channel.
3. Influence of antenna can be decoupled from channel model, thus different antenna types can be used for same channel.

Some of widely accepted GSCM falls under family of COST (COST 259 [27] [28], 273 [29] and 2100 [30]), WINNER [31] and 3GPP Spatial Channel Model (SCM) [32].

In this thesis work, we choose WINNER2 channel model for simulation purposes. This is mainly because of the above mentioned advantages of GMSC and also open source code is available by WINNER group for simulating WINNER2 channel in MATLAB. However, WINNER2 channel model doesn't consider the effect of diffuse scattering. Also, WINNER2 model is a drop based model as a consequence, it is not possible to perform changing channel conditions simulations, where inaccuracies caused by movement of UE is not included.

3.3 WINNER2 channel

WINNER+ (Wireless World Initiative New Radio+) is a consortium of 29 partners to develop, optimize and evaluate International Mobile Telecommunications (IMT), one of their project was WINNER2 channel model, used for link and system level simulations of local, metropolitan and wide area wireless communications scenarios [31].

WINNER2 channel model supports any wireless system working in 2-6 GHz frequency range with up to 100 MHz bandwidth. In addition, it supports 17 different propagation scenarios and multiple antennas technologies. As mentioned earlier, the WINNER2 model was mainly chosen due to the fact that, for this thesis, a geometry-based stochastic channel model is required, creating what is called the double directional radio channel model.

Basically, the channel generation considers the configuration of Bs, UE antennas and positions, and the chosen scenario. Based on that, the channel parameters are chosen from statistical distributions derived from extensive campaign measurements done by the WINNER+ team. Then, the final channel realizations are only the sum of different MPCs reflected from numerous scatterers generated randomly in the simulated environment. Noting that the channel parameters are constant within each channel snapshot also known as a drop. Plus, scatterers in the environment that falls into the same region form a cluster, the number of clusters is relevant to the scenario being simulated, and the rays reflected from a certain cluster share the same delay, power, AOA, and Angle of Departure (AOD) values as shown in figure 9. So, the channel from Transmitter antenna element s to receiver element u for each cluster n is written as

$$\begin{aligned}
H_{u,s,n}(t;\tau) = \sum_{m=1}^M & \begin{bmatrix} F_{rx,u,V}(\varphi_{n,m}) \\ F_{rx,u,H}(\varphi_{n,m}) \end{bmatrix}^T \begin{bmatrix} \alpha_{n,m,VV} & \alpha_{n,m,VH} \\ \alpha_{n,m,HV} & \alpha_{n,m,HH} \end{bmatrix} \begin{bmatrix} F_{tx,s,V}(\phi_{n,m}) \\ F_{tx,s,H}(\phi_{n,m}) \end{bmatrix} \\
& \times \exp(j2\pi\lambda_0^{-1}(\bar{\varphi}_{n,m} \cdot \bar{r}_{rx,u})) \exp(j2\pi\lambda_0^{-1}(\bar{\phi}_{n,m} \cdot \bar{r}_{tx,s})) \\
& \times \exp(j2\pi\nu_{n,m}t)\delta(\tau - \tau_{n,m}),
\end{aligned}$$

where $F_{rx,u,V}$ and $F_{rx,u,H}$ are the Rx antenna array u field patterns for the vertical and horizontal polarizations respectively, $\alpha_{n,m,VV}$ and $\alpha_{n,m,VH}$ are the gains of vertical to vertical and horizontal to vertical polarizations of ray n, m respectively. Plus, λ_0 is the wavelength of the carrier frequency, $\phi_{n,m}$ and $\varphi_{n,m}$

- Angles of Arrival (AOA).
- Angles of Departure (AOD).
- Path Delays and Powers.
- Initial phases of the rays.

The channel parameters could be generated as in the steps below:

1. Assign the propagation scenario and the environment parameters such as, number of BSs antennas, UEs and their configurations and many more parameters that will be discussed in the simulation section.
2. Set the propagation (LOS/NLOS) condition, by using defined functions of distance for each scenario, that sets the probability of having LOS case.
3. Determine the pathloss for each link between the BS and UE, the pathloss values are calculated from predefined equations obtained from the measurement campaign.
4. Create the large scale parameters mentioned above.
5. Create the path delays τ , which can be considered as random variables with exponential distribution (except for Urban micro-cell NLOS case, normal distribution is used), characterized by the delay spread which is different for each scenario. The delays must be normalized by subtracting the minimum delay and then sort the normalized delays in a descending order.
6. Create the cluster powers P , where a single slope exponential power delay profile is assumed, the power is related to the delay distribution used when generating the path delays, the shadow fading is included, and it is drawn from given table, that has different values for each scenario. It should be noted that the power is normalized so that the sum of all clusters power is equal to 1. Plus, since each cluster consists of number of rays, the cluster power is divided by the number of rays that form the cluster, so that, all rays within a cluster have equal powers.
7. Generate AOAs and AODs, since the Angular Spread (AS) is considered to be wrapped Gaussian distributed, the AOAs or AODs can be determined by the inverse Gaussian function that relies on the angular spread, cluster power and some scaling factor related to total number of clusters, then, the generated angles are multiplied with a random variable to assign random signs. In the LOS case the first the cluster is enforced to the LOS direction obtained from the geometrical settings of the UE and BS.
8. Randomly link of rays within a cluster, after the AOAs and AODs were generated, the departure ray angles are coupled randomly to the arrival ray angles in each cluster.
9. Create the cross polarization of the power ratios.

10. Generate the random initial phases for each ray in each cluster, which are uniformly distributed between $[-\pi, \pi]$.
11. The channel coefficients is generated as per WINNER2 channel model equation.

3.3.2 Propagation scenarios

The WINNER2 model supports 17 propagation scenarios which cover typical cases like rural, urban, dense urban, indoor office, large indoor, fast moving train etc. It doesn't cover all possible scenarios conditions like mountain or hilly rural. However, Since rural and urban are the most common propagation scenarios in mobile communication, we will concentrate on these two scenarios. However, the MATLAB LTE model supports other scenarios as well. Next, we will describe briefly these two scenarios.

1. B1 - Urban micro-cell
In Urban micro-cell the BS and UE are placed well below surrounding buildings. There is a main street where BS and UE have LOS communication but may be interrupted by traffic in the street. Then, there are many other streets which are perpendicular to the main street, hence, they have NLOS communication. The Cell radius is up-to 5 km and UE velocity can vary from 0 to 70 km/h.
2. D1 - Rural macro-cell
In Rural macro-cell, the BSs are placed well above surrounding buildings heights. Thus, LOS condition can be assumed in most cases. Cell radius is up-to 10km and UE velocity can vary from 0 to 200 km/h.

3.3.3 FDD modeling

In general, the WINNER2 channel model code is only designed to create the downlink channel by default, but, since thesis is based on estimating downlink the beamforming weights based on the uplink channel measurements for FDD system. So, there is a need for creating the uplink channel also.

It is observed that large scale parameters show frequency dependence. While, most of small scale parameters like AOA, AOD, path delays , and path powers are considered invariant with frequency change [6]. Based on this assumption, the uplink channel is created as per steps explained below. For full duplex channel with duplex gap of Δf_c Hz and uplink frequency of f_{ul} Hz [31].

1. Generate the downlink channel at carrier frequency $f_{ul} + \Delta f_c$ Hz.
2. Save the small scale parameters.
3. Again generate the downlink channel at carrier frequency f_{ul} as follow.
 - Using the saved small scale parameters.
 - Randomize the initial phase of rays.

4. The Uplink channel can be created by taking the transpose of the channel created in step 3.

3.3.4 Path loss model

The most simple path loss model is free space path loss model, which only depends upon distance and frequency, But it has been observed that path loss also depends on other parameters, like buildings' heights, BS, UE heights and other environment's factors which are hard to model so, most of the path loss models are based on the actual channel measurements. In The WINNER2 the following path loss model is used

$$PL = A \log_{10}(d) + B + C \log_{10} \left(\frac{f_c}{5} \right) + X, \quad (1)$$

where $d[m]$ is distance in meter f_c carrier frequency in GHz. Parameter A,B,C and X are environment dependent and are given in [31].

3.3.5 Shadow fading

In addition to the path loss, there is shadow fading effect as well. This effect occurs when the UE is moving and gets covered by a high rise obstacle like building or hill for some time. This range of movement can be from few meters up-to several hundred meters. Many experimental investigations show that shadow fading can be modeled by log-normal distributed. In the WINNER2 channel model, the standard deviation for each scenario is given and can be found in [31].

3.3.6 Ricean factor

In LOS case, most of the time there are weak NOLS components along with dominant LOS component. Many experimental investigations show that distribution of amplitude in such conditions shows Ricean distribution. The ratio of power between LOS and NLOS component is called Ricean factor K_r . This is scenario dependent and is given in the WINNER2 model and can be found in [31].

3.3.7 Coherence time

Characteristics of wireless channel change because of relative motion between UE and BS, or by movement of intermediate objects in channel, time over which impulse response of channel remains invariant is known as coherence time. This is an important parameter, as it determines how often BS need to compute channel weights for each user. If coherence time is defined as time over which the time correlation function of channel is greater than 0.5, then coherence time is given by [33].

$$T_c \approx \frac{9}{16\pi f_d}, \quad (2)$$

where f_d is maximum Doppler shift. Figure 10 gives the snapshots of frequency transfer function at center frequency of channel in time domain for 0.1 second. However, Doppler shift can also be caused by movement of intermediate objects, but, in WINNER2 model for B1 and D1 scenario Doppler shift is calculated from AOA(downlink) ($\phi_{n,m}$) UE speed (v) and direction of travel of UE (θ_v)

$$f_d = \frac{\|v\| \cos(\phi_{n,m} - \theta_v)}{\lambda}. \quad (3)$$

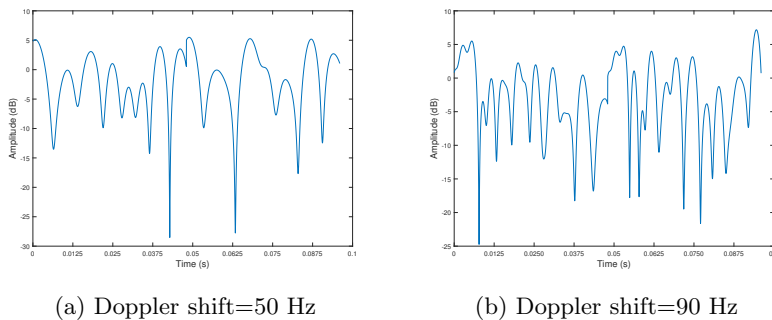


Figure 10: The effect of Doppler spread on the channel frequency transfer function at center frequency.

3.3.8 Coherence bandwidth

The wireless channel also varies with frequency of the signal because of MPC. The Coherence bandwidth can be defined as frequency range over which channel can be considered flat. The Coherence bandwidth can directly determine the frequency range over which same channel weights can be used. If the coherence bandwidth is defined as frequency over which frequency correlation function of channel is greater than 0.5, then, the coherence bandwidth is given by [33]

$$B_c = \frac{1}{5S_\tau}, \quad (4)$$

where S_τ is RMS delay spread. In the WINNER2, the number of MPCs for each scenario is given and can be found in [31]. Corresponding delays and cluster powers are drawn randomly as per distribution.

3.4 Noise

For a reliable communication, signal power should be greater than interference plus noise power. While interference can be controlled by using different duplexing (time, frequency and space) techniques, noise power in most cases is unavoidable. Broadly there are three types of noise which can occur in communication systems [6]:

1. Thermal noise.
2. Man-made noise.
3. Receiver noise.

In this thesis, only thermal noise which is flat over a given bandwidth (B) will be considered and the thermal noise power is given by [6].

$$N = K_B T_e B, \quad (5)$$

where K_B is Boltzmann's constant and T_e is the equivalent temperature in Kelvin. In this thesis we choose $T_e = 300\text{K}$.

3.5 Uplink and downlink channel representation

In a wireless channel, a transmitted signal is reflected by multiple objects such as buildings, stationary or moving vehicles before the receiver senses the transmitted signal. This give rise to multiple copies of transmitted signal which are commonly known as MPCs. In spatial domain, each path can be characterized by AOA, path gain, phase and delay. For uplink, received signal at the BS can be written as

$$\mathbf{x}(t) = \sum_{k=1}^N \sum_{l=1}^{L_k} \mathbf{h}_{u,k}^{(l)}(t) s_{u,k}(t - \tau_{u,k}^{(l)}) + \mathbf{n}(t), \quad (6)$$

where:

$s_{u,k}(t)$ is the signal transmitted from the UE k .

$\mathbf{h}_{u,k}^{(l)}$ is an $M \times 1$ vector of the l th path channel response of the UE k .

$\tau_{u,k}^{(l)}$ is the l th time delay of the UE k .

L_k is the number of resolvable delay path for the UE k .

$\mathbf{n}(t)$ is an $M \times 1$ noise vector.

$\mathbf{x}(t)$ is an $M \times 1$ received signal vector at the BS,

here subscript u represents uplink.

For downlink each user will have its own received signal and is given by

$$\mathbf{r}_k(t) = \sum_{j=1}^N \sum_{l=1}^{L_k} \mathbf{w}_j^H \mathbf{h}_{d,k}^{(l)}(t) s_{d,j}(t - \tau_{d,k}^{(l)}) + \mathbf{n}_k(t), \quad (7)$$

where:

$\mathbf{r}_k(t)$ is the received signal by the UE k .

$\mathbf{w}_j^{(H)}$ is a $1 \times M$ downlink beamforming weight for j .

$s_{d,k}(t)$ is the signal transmitted to the UE k .

$h_{d,k}^{(l)}$ is an $M \times 1$ vector for the l th path channel response of the UE k .

$\tau_{d,k}^{(l)}$ is the l th time delay for the UE k .

L_k is the number of resolvable delay paths for the UE k .

$\mathbf{n}_k(t)$ is an AWGN noise vector at the UE k .

\mathbf{N} is the total number of users which are beamformed.

To construct the uplink channel response for user k , consider the l th MPC having an AOA $\theta_{k,l}$. The uplink array response vector for the k th user, $\mathbf{a}_{u,k,l}(\theta_{k,l})$ for the signal arriving from the l th path is given by

$$\mathbf{a}_{u,k,l}(\theta_{k,l}) = [1, e^{j2\pi \sin(\theta_{k,l})/\lambda_u}, \dots, e^{j2(m-1)\pi \sin(\theta_{k,l})/\lambda_u}], \quad (8)$$

while the uplink channel response for the k th user is given by

$$\mathbf{h}_{u,k}(t, \tau) = \sum_{l=1}^{L_k} f(\theta_l) \alpha_{u,k,l}(t) \mathbf{a}_{u,k,l}(\theta_{k,l}) \delta(t - \tau_{k,l}(t)), \quad (9)$$

where $f(\theta)$ is the transmit and receive gain patterns of BS antennas. Suppose the cell is divided into S sectors, then, for a given sector $f(\theta)$ is zero outside that sector ie.:

$$\begin{aligned} f^2(\theta) &\neq 0, -\pi/S \leq \theta \leq \pi/S, \\ f^2(\theta) &= 0 \text{ otherwise.} \end{aligned} \quad (10)$$

Note $\alpha_{u,k,l}(t) = K_{u,k,l} \tilde{\alpha}_{u,k,l}$, Where $K_{u,k,l}$ is the combined uplink shadow fading and the path loss parameters for user k path l , and $\tilde{\alpha}_{u,k,l}$ accounts for the uplink fast fading.

For FDD systems, AOA and AOD are the same, since they are invariant for change in frequency, while other parameters change with frequency. So, downlink channel response can be written as

$$\mathbf{h}_{d,k}(t, \tau) = \sum_{l=1}^{L_k} f(\theta_l) \alpha_{d,k,l}(t) \mathbf{a}_{d,k,l}(\theta_{k,l}) \delta(t - \tau_{k,l}(t)), \quad (11)$$

where $\mathbf{a}_{d,k,l}(\theta_{k,l})$ is the downlink array response vector for the k th user for the signal arriving from the l th path and is given by

$$\mathbf{a}_{d,k,l}(\theta_{k,l}) = [1, e^{j2\pi \sin(\theta_{k,l})/\lambda_d}, \dots, e^{j2(m-1)\pi \sin(\theta_{k,l})/\lambda_d}], \quad (12)$$

note $\alpha_{d,k,l}(t) = K_{d,k,l} \tilde{\alpha}_{d,k,l}$, where $K_{d,k,l}$ is the combined downlink shadow fading and the path loss parameters for user k path l and $\tilde{\alpha}_{d,k,l}$ accounts for the downlink fast fading.

When we analyze the parameters in equation 9 and 11, we can see that for an FDD system, they differ in terms of shadow fading, path loss, fast fading and array response. While shadow fading, path loss and array response are deterministic, fast fading is completely random hence indeterministic. The uplink covariance channel matrix (UCCM) and downlink covariance channel matrix (DCCM) can be calculated by taking the expected value of the uplink and downlink channel response for long enough time, so the fast fading is averaged out but shorter than the coherence time of the channel. Thus, UCCM and DCCM for the K^{th} user can be expressed as

$$\mathbf{R}_{u,k} = \sum_{l=1}^{L_k} f^2(\theta_l) \mathbb{E} [\alpha_{u,k,l}^2] \mathbf{a}_{u,k,l}(\theta_{k,l}) \mathbf{a}_{u,k,l}^H(\theta_{k,l}), \quad (13)$$

$$\mathbf{R}_{d,k} = \sum_{l=1}^{L_k} f^2(\theta_l) \mathbb{E} [\alpha_{d,k,l}^2] \mathbf{a}_{d,k,l}(\theta_{k,l}) \mathbf{a}_{d,k,l}^H(\theta_{k,l}). \quad (14)$$

4 Beamforming

4.1 Introduction

Beamforming is a signal processing technique used in MIMO systems, where the transmitter and the receiver utilize the channel information to focus energy in a particular direction, in order to maximize the received signal energy, and introduce minimum interference between different users.

In mobile networks, broadly there are two types of beamforming techniques, mainly transmitter side and receiver side beamforming can be implemented. The receiver side beamforming can only affect the signal quality of one user, this happens when the receiver with multiple antennas adjusts the weights for the receiving antennas to maximize the received power, meanwhile the transmitter side beamforming is more complex because the signal from the transmitter is received not only by the desired user but also by other users. Another major difference between transmitter and receiver side beamforming is that, in receiver side beamforming, the receiver can estimate the channel either from training data or by a blind method, while in transmitter side beamforming, the transmitter has to rely on channel reciprocity or feedback from the receiver for channel estimation. As per the scope of the thesis, from now on in the report, beamforming will refer to as transmitter side beamforming.

As mentioned in section 2.6.1, MU-MIMO can increase spectral efficiency. However, since transmitting in the downlink for multiple users using the same frequency bandwidth yields high interference, and almost total error in the received messages, MU-MIMO is applicable only due to some kind of processing done from the base station side, the transmitted signal from the BS can be represented as

$$\mathbf{z} = \mathbf{W}\sqrt{\mathbf{P}_d}\mathbf{s}, \quad (15)$$

where W is the precoding matrix (Beam weights), which maps the symbols to the M transmitting antennas, \mathbf{P}_d contains the power allocation for the different K users, with $P_i, i = 1, 2 \dots, K$ on its diagonal, and \mathbf{s} is the transmitted symbols for the K users, where each entry has unit energy. Nonetheless, the precoding matrix must be normalized in power so it will not add any power. In mathematical notation we can say,

$$\mathbb{E} \|\mathbf{z}\|^2 = 1 \Rightarrow \text{Tr} \left\{ \mathbf{P}\mathbf{W}^H\mathbf{W} \right\} = 1,$$

meanwhile, the received vector by the K users will be

$$\mathbf{y} = \sqrt{\mathbf{P}_d}\mathbf{H}\mathbf{W}\mathbf{s} + \mathbf{n}, \quad (16)$$

where \mathbf{H} is the channel matrix and \mathbf{n} is the white noise vector with complex Gaussian elements that has zero mean and variance σ_n^2 . So, \mathbf{W} will be chosen to fulfill certain objective, in this section we will only describe the beamforming methods used in our thesis work.

4.2 Beamforming techniques

As mentioned earlier, the precoding matrix is chosen in such a way that satisfies a certain requirement. In most of the literature, three objective functions arise when calculating the beamforming weights, and those will be discussed in this section.

4.2.1 Matched filtering (MF)

Also known as Maximum Ratio Transmission (MRT), it is a simple linear precoding technique, which objective is to maximize SNR for each user. So, the problem we have is,

$$\mathbf{W}_{MF} = \arg \max_W \frac{\mathbb{E} \|\mathbf{P}_d \mathbf{H} \mathbf{z}\|^2}{\sigma_n^2} \text{ s.t. } \text{Tr} \{ \mathbf{P} \mathbf{W}^H \mathbf{W} \} = 1,$$

the solution as shown in [34] is given by

$$\mathbf{W}_{MF} = \mathbf{H}^H,$$

therefore, the received signal by user k will be

$$\mathbf{y}_k = \sqrt{\mathbf{P}_d} \mathbf{h}_{d,k} \mathbf{h}_{d,k}^H \mathbf{s}_k + \sqrt{\mathbf{P}_d} \sum_{\substack{j=1 \\ j \neq k}}^K \mathbf{h}_{d,k} \mathbf{h}_{d,j}^H \mathbf{s}_j + \mathbf{n}_k, \quad (17)$$

where \mathbf{h}_k is the channel response vector between BS antennas and the user k .

It is clear that MRT do not take into consideration the interference effect of other users, even though it is a simple process of matrix hermitian, it is not very suitable for multiple users and high SNR scenarios.

4.2.2 Zero forcing (ZF)

Another linear technique, has more robust performance in terms of providing better user separation over the MRT, as it takes into consideration the interference effect from other users, when calculating the beam weights \mathbf{W} , the optimization problem is given by

$$\mathbf{W}_{ZF} = \arg \min_W \mathbb{E} \left\{ \|\mathbf{W} \sqrt{\mathbf{P}} \mathbf{x}\|^2 \right\} \text{ s.t. } \mathbf{h}_k \mathbf{w}_j = 0 \text{ for } j \neq k.$$

In other words, minimize transmitted power and choose \mathbf{W} to cancel the channel effect of each user, as a result, each user will be able to separate its own stream without interference from others. The solution as shown in [35] is the pseudo inverse of the channel matrix given by

$$\mathbf{W}_{ZF} = \mathbf{H}^\dagger = \mathbf{H}^H (\mathbf{H} \mathbf{H}^H)^{-1},$$

and the the received signal by the user k is

$$\mathbf{y}_k = \sqrt{P_d} \mathbf{s}_k + \mathbf{H}^\dagger \mathbf{n}. \quad (18)$$

However, it must be noted that the ZF precoding is only possible when $M_T > KM_R$, that is, to obtain an inverse of the channel \mathbf{H} , the number of transmitting antennas must be bigger than the number of users multiplied with the number of antennas per user terminal.

4.2.3 Regularized zero forcing (RZF)

One problem encountered when using ZF precoding is due to the channel inverse when the channel is not full rank. This results in high condition number which represents the ratio between the highest eigenvalue to the smallest one, another known term is almost singular matrix. This problem is reflected in the minimization problem in 4.2.2, when the objective is to minimize the transmitted power, however, due to the ill conditioned channel matrix, the term $(\mathbf{H}\mathbf{H}^H)^{-1}$ will be large, to compensate that, the power assigned to the users must be decreased which results in degradation in the performance of the ZF.

To solve this problem, the RZF can be used, which is a linear precoding, and it is a trade-off between the high power of the MRT and the interference cancellation of the ZF, it basically takes into consideration the noise and tries to minimize the difference between the transmitted signal and the received ones, that is why it is also referred to as MMSE, the solution as shown in [26] is given by

$$\mathbf{W}_{RZF} = \mathbf{H}^H (\mathbf{H}\mathbf{H}^H + \alpha \mathbf{I})^{-1},$$

where $\alpha = \frac{K\sigma_n^2}{P_d}$ is a regularization parameter, it is clear that in the case that $\alpha = 0$, corresponding to high SNR, RZF will converge to ZF, meanwhile for $\alpha = \infty$, corresponding to low SNR, RZF converges to MRT [26].

4.3 Beamforming in LTE

Generally, depending upon the coherence time and the bandwidth, the same beamforming weights (\mathbf{W}) are used for multiple resource elements. However, in this thesis, beamforming weights are calculated for each subframe, each subframe further have 14 OFDM symbols. The received signal by the K users from the M BS antennas can be expressed as

$$\mathbf{y}(s) = \mathbf{H}_d(s) \mathbf{W} \mathbf{s}(s) + \mathbf{n},$$

where s here represents the index number in the resource grid. For example, in a 20 MHz BW channel we have 1200 subcarriers in each OFDM symbol, so, in total we have 16800 (1200×14) indices, the idea is to find the beamforming weights \mathbf{W} for each subframe at a time, and then weight symbols for all users $\mathbf{s}(s)$ to all BS antennas $\mathbf{A}(s)$ using

$$\mathbf{A}(s) = \mathbf{W} \mathbf{s}(s),$$

$$\begin{bmatrix} a_1(s) \\ a_2(s) \\ \vdots \\ a_M(s) \end{bmatrix} = \begin{bmatrix} w_{1,1} & \cdots & w_{1,K} \\ w_{2,1} & \cdots & w_{2,K} \\ \vdots & \ddots & \vdots \\ w_{M,1} & \cdots & w_{M,K} \end{bmatrix} \begin{bmatrix} s_1(s) \\ s_2(s) \\ \vdots \\ s_K(s) \end{bmatrix},$$

the weighted signal received by all UEs transmitted by the BS antennas over the channel is given by

$$\mathbf{y}(s) = \mathbf{H}_d(s)\mathbf{a}(s) + \mathbf{n},$$

$$\begin{bmatrix} u_1(s) \\ u_2(s) \\ \vdots \\ u_K(s) \end{bmatrix} = \begin{bmatrix} h_{1,1}(s) & \cdots & h_{1,M}(s) \\ h_{2,1}(s) & \cdots & h_{2,M}(s) \\ \vdots & \ddots & \vdots \\ h_{K,1}(s) & \cdots & h_{K,M}(s) \end{bmatrix} \begin{bmatrix} a_1(s) \\ a_2(s) \\ \vdots \\ a_M(s) \end{bmatrix}.$$

4.4 Beamforming in time division duplex systems

In TDD systems, the uplink is separated from the downlink by allocating different time slots in the same frequency band, this results in the same spatial signature of the channel in both uplink and downlink, thus, the BS can estimate the downlink channel by reciprocating the measured uplink channel, provided that the time difference between the uplink and the downlink is less than the coherence time of the channel, as shown in figure 11. If the duplexing time is greater than the coherence time, then still, the downlink channel can be estimated by averaging out the fast fading, this can be achieved by averaging the instantaneous uplink measured channel for a long enough time that the fast fading is averaged out, but shorter enough that the shadow fading and the main AOA remains the same, as shown in figure 12 [36].

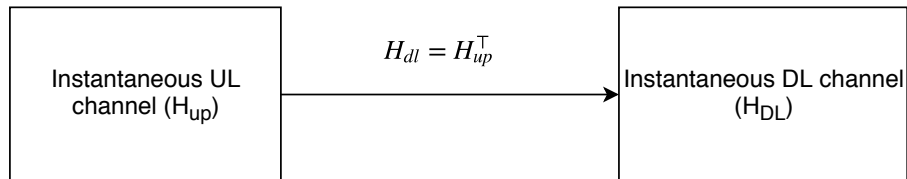


Figure 11: TDD for short duplex time.

4.5 Beamforming in frequency division duplex systems

In FDD systems, the uplink is separated from the downlink by different frequency band, but during the same time interval. This results in different spatial signature of the channel in uplink and downlink if the duplexing bandwidth is larger than the coherence bandwidth of the channel, so, to estimate the downlink channel from the uplink channel measurements, we need to first average out

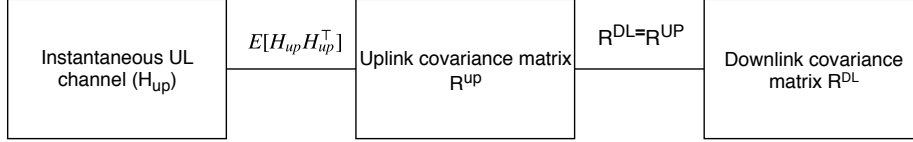


Figure 12: TDD for long duplex time.



Figure 13: FDD for long duplex time.

small scale fading, and then apply some frequency transformation techniques as explained in figure 13. This is known as open loop beamforming.

There are other methods in which user estimates the downlink channel and feeds it back to the BS, this is known as closed loop beamforming, it is more accurate than open loop beamforming, but it suffers from high feedback overhead, for example, if the BS with M antennas serves K single antenna users, then, total feedback overhead will be $M + K$ symbols, as explained in [8], for $M = 100$ and $K = 25$ FDD operation cannot be supported even by spending 50% of the uplink resources. Various research groups have proposed methods to reduce pilot overheads for FDD systems, but as per thesis scope, they will not be described further, and only open loop methods will be discussed. Researchers have proposed different methods for open loop beamforming, some of them are explained in details below.

4.5.1 Matched array

This is a hardware based approach in which the position of antennas array is designed in such a way that it minimizes the difference between the transmit and the received response [37], this can be done by placing two separate closely located arrays with each having similar response, or design a single array which minimizes the difference between responses.

4.5.2 Directional based transformation

Directional based transformation is based on the idea that the AOA and the AOD are invariant of frequency transformation, thus remains conserved [9] [10]. Here, the BS applies downlink beamforming in the direction of uplink dominant AOA [4]. The idea can be further extended to 2-D array where the BS estimates both azimuthal and vertical AOAs [38] [39].

Subspace based algorithms like multiple signal classification (MUSIC) is among popular AOA estimation algorithm because of its relatively high resolution [40]. However, it has been observed that in a dense urban environment, the measured angular spread can be between 3° to 20° [6], under such conditions, the robustness of AOA based techniques highly degrades.

4.5.2.1 1-D Angle-of-Arrival based beamforming

The AOA based beamforming used in this thesis is based on the work proposed in [4]. The idea is to estimate downlink channel based on the dominant AOA for each user, and then use ZF, RZF, and MRT for calculating beamforming weights. For BS antennas with uniform gain pattern within its sector, from equation 9, the time varying 2-D uplink channel impulse response for the k^{th} user is given by

$$\mathbf{h}_{u,k}(t, \tau) = \sum_{l=1}^{L_k} \alpha_{u,k,l}(t) \mathbf{a}_{u,k,l}(\theta_{k,l}) \delta(t - \tau_{k,l}(t)). \quad (19)$$

Since the uplink channel impulse response contains AOA information, the AOA of each MPC can be estimated. The algorithm which is used to estimate AOA in this thesis is MUSIC [40].

Only one MPC with the highest power is selected for each user, this is done by selecting the AOA with the highest power. After that, the downlink channel response is estimated by using only this information while ignoring other parameters, and this is given by

$$\mathbf{H}_d = [\mathbf{a}(\theta_{1,dom}), \mathbf{a}(\theta_{2,dom}), \dots, \mathbf{a}(\theta_{N,dom})],^H \quad (20)$$

where N is the number of users to be beamformed. So, the weights are calculated using ZF, RZF, and MRT as described in section 4.2.

4.5.3 Covariance matrix transformation

As explained in section 4.4, the uplink covariance matrix can be estimated by averaging the instantaneous uplink channel matrix, after that, some frequency transformation techniques can be applied to obtain downlink covariance matrix, some suggestions are to use Capon method or Frequency Calibration algorithm (FC) which will be discussed in details next.

4.5.3.1 Capon beamformer

This method relies on covariance matrix transformation and it was proposed in [12], as mentioned in section 3.5, the uplink received signal at the BS and the UCCM are given by, (restated here for convenience)

$$\mathbf{x}(t) = \sum_{k=1}^N \sum_{l=1}^{L_k} \mathbf{h}_{u,k}^{(l)}(t) s_{u,k}(t - \tau_{u,k}^{(l)}) + \mathbf{n}(t),$$

$$\mathbf{R}_{u,k} = \sum_{l=1}^{L_k} f^2(\theta_l) \mathbb{E} [\alpha_{u,k,l}^2] \mathbf{a}_{u,k,l}(\theta_{k,l}) \mathbf{a}_{u,k,l}^H(\theta_{k,l}),$$

while the spatial covariance matrix for interference plus noise is written as

$$\mathbf{Q}_{u,k} = \sum_{i \neq k} \mathbf{R}_i + \sigma_N^2 \mathbf{I}, \quad (21)$$

where σ_N^2 denotes the noise variance and \mathbf{I} is the identity matrix. Using this information, the beamforming weights can be calculated as a solution for the optimization problem called Optimum Combining [41], which maximizes the SINR for each user and it is given by

$$\mathbf{W}_k = \arg \max_W \text{SINR}_k = \arg \max_W \frac{\mathbf{W}^H \mathbf{R}_k \mathbf{W}}{\mathbf{W}^H \mathbf{Q}_k \mathbf{W}}. \quad (22)$$

However, since in FDD, the channel reciprocity assumption is violated, using the weights that were calculated from the uplink data is not valid, due to the uncorrelated fading and the frequency dependent array vector between the uplink and the downlink as mentioned earlier, and this where the spatial covariance matrix transformation (SCMT) is applied, figure 14 shows the steps this method goes through to obtain the DCCM and corresponding steps are described in detail below.

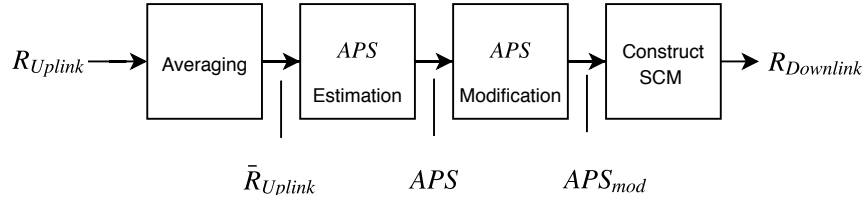


Figure 14: Capon spatial covariance transformation steps, source [12].

1. Averaging for UCCM is performed, to reduce the effect of the uncorrelated fading between the uplink and the downlink.
2. Estimate the APS for each user by using the minimum variance distortion less response filter, known as Capon beamformer [42]. The estimated APS for the user k is given by

$$\hat{\mathbf{P}}_k(\theta) = \frac{1}{\mathbf{a}_u^H(\theta) \mathbf{R}_{u,k}^{-1} \mathbf{a}_u(\theta)}. \quad (23)$$

3. In order to reduce interference, APS is modified by weighting the user APS with a rectangular window centered at $\theta_{k,dom}$, which is the APS dominant

peak for user k , this will be used for calculating $\mathbf{R}_{d,k}$. Meanwhile, the APS of the interference is assumed to be the rest of the APS that was not weighted in the rectangular window. The APS modification steps are given by

$$P_{k,mod}(\theta) = P_k(\theta)rect[\theta_{k,dom} - \xi, \theta_{k,dom} + \xi], \quad (24)$$

$$P_{k,int}(\theta) = P_k(\theta)(1 - rect[\theta_{k,dom} - \xi, \theta_{k,dom} + \xi]), \quad (25)$$

where 2ξ denotes the reshaping rectangular window width, in this thesis work, the window width was chosen where the peak power of the user APS drops 3 dB, figure 15 better explains the concept above, it shows how the window (dotted black) is taken around the peak of the APS for a certain user, and what is inside the window will be used for covariance matrix calculation. The remaining part will be used for what is assumed to be interference. It is worth mentioning that this method set nulls not only where there is interference from other users, but rather everywhere except for the user's peak window.

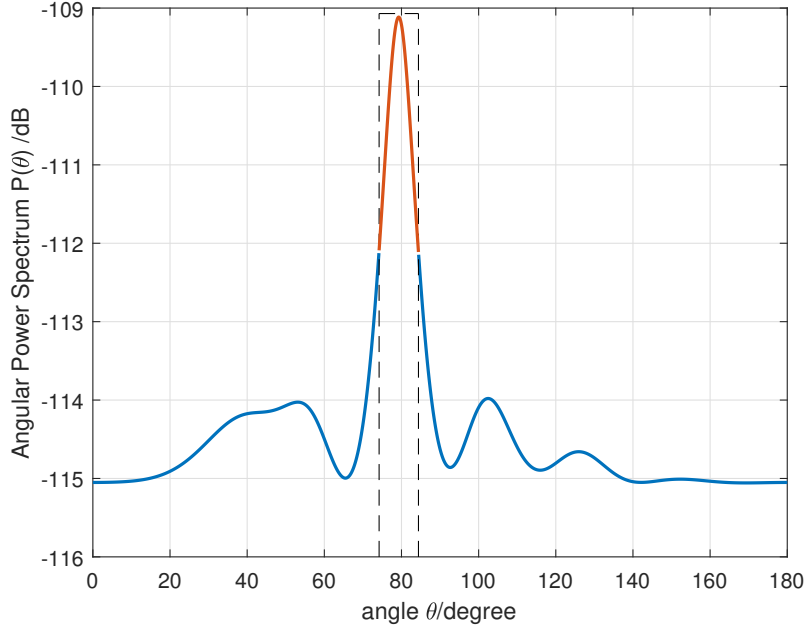


Figure 15: APS Modification by the weighting window (dotted black), red part will be used to calculate covariance matrix, the rest is assumed to be interference.

4. Now, the DCCM can be written as

$$\mathbf{R}_{d,k} = \int_{\theta} P_{k,mod}(\theta) \mathbf{a}_d(\theta) \mathbf{a}_d^H(\theta) d\theta, \quad (26)$$

likewise, the spatial covariance matrix for what is assumed as interference is constructed as

$$\mathbf{Q}_{d,k} = \int_{\theta} P_{k,int}(\theta) \mathbf{a}_d(\theta) \mathbf{a}_d^H(\theta) d\theta. \quad (27)$$

Finally, the weights can be calculated as stated in equation 22. However, the generalized eigenvector of $\mathbf{R}_{d,k} \mathbf{Q}_{d,k}$ that is used in [12], has not shown robust performance in terms of SINR, and there are lot papers that deal with finding a robust solution for equation 22. Nonetheless, we obtained better results when using the minimum variance beamformer (MVB) as shown in [42] as the optimal solution is given by

$$\mathbf{W}_k = \frac{\mathbf{R}_{y,k}^{-1} \mathbf{a}_u}{\mathbf{a}_u^H(\theta) \mathbf{R}_{y,k}^{-1} \mathbf{a}_u(\theta)}, \quad (28)$$

where $\mathbf{R}_{y,k} = \mathbf{R}_{d,k} + \mathbf{Q}_{d,k}$, which corresponds to the estimated covariance of the received signal by the user.

In conclusion, the array vector could be different from the actual value, mainly because of inaccurate estimation of the angle of arrival, this will lead to erroneous beamforming weights calculation [43]. Therefore, this method also depends on the angle of arrival even though, it relies on SCMT method.

4.5.3.2 FC algorithm

FC Algorithm does not calculate the AOA directly, however, it relies on the AOA reciprocity. It is based on calculating DCCM through UCCM using frequency calibration (FC) matrix, FC algorithm was proposed in [13]. It is assumed that the rays from the same MPC have uniform distribution in interval $[\phi - \Delta/2, \phi + \Delta/2]$, where ϕ is the nominal AOA and Δ is the angular spread, assuming the path loss and the shadow fading are invariant in the uplink and the downlink, we obtain $\mathbb{E}[\alpha_{u,i}^2] = \mathbb{E}[\alpha_{d,i}^2] = |\alpha_i|^2$. Thus, from equation 13 and 14 the UCCM and the DCCM corresponding to user k can be written as

$$\mathbf{R}_u = \sum_{i=1}^P f^2(\theta_i) \alpha_i^2 \mathbf{a}_u(\theta_i) \mathbf{a}_u^H(\theta_i), \quad (29)$$

$$\mathbf{R}_d = \sum_{i=1}^P f^2(\theta_i) \alpha_i^2 \mathbf{a}_d(\theta_i) \mathbf{a}_d^H(\theta_i). \quad (30)$$

When comparing the above two equations, we observe that they only differ in the steering vector term. Now we briefly summarize the algorithm 1 proposed in [13], which was used in this thesis to estimate the DCCM from the UCCM

1. Each cell is divided into three sectors, thus, each sector covers 120°

2. Compute \mathbf{Q}_u^l and \mathbf{Q}_d^l for $l = -L, -L + 1, \dots, L$ using

$$\mathbf{Q}_u^l = \sum_{\theta=-60^\circ}^{60^\circ} \mathbf{a}_u(\theta) \mathbf{a}_u^H(\theta) e^{-jlS\theta}, \quad (31)$$

$$\mathbf{Q}_d^l = \sum_{\theta=-60^\circ}^{60^\circ} \mathbf{a}_d(\theta) \mathbf{a}_d^H(\theta) e^{-jlS\theta}, \quad (32)$$

where $L = M-1$ as M is the number of BS antennas and $S=3$.

3. Construct \mathbf{Q}_u and \mathbf{Q}_d using

$$\mathbf{Q}_u = \left[\mathbf{Q}_u^{-L}(\cdot), \mathbf{Q}_u^{-L+1}(\cdot), \dots, \mathbf{Q}_u^L(\cdot) \right], \quad (33)$$

$$\mathbf{Q}_d = \left[\mathbf{Q}_d^{-L}(\cdot), \mathbf{Q}_d^{-L+1}(\cdot), \dots, \mathbf{Q}_d^L(\cdot) \right]. \quad (34)$$

For an $m \times n$ matrix \mathbf{X} , $\mathbf{X}(\cdot)$ denotes the $mn \times 1$ vector whose elements are taken column wise from matrix \mathbf{X} .

4. Now, we construct the FC matrix \mathbf{A} of dimension $M^2 \times M^2$ via

$$\mathbf{A} = \mathbf{Q}_d (\mathbf{Q}_u^H \mathbf{Q}_u)^{-1} \mathbf{Q}_u^H. \quad (35)$$

Note, since the FC matrix depends only on uplink/downlink frequency, the BS antennas geometry and the cell sector, so, it can be computed once and stored in advance.

5. Use the uplink channel response to compute the UCCM, then \mathbf{r}_u and \mathbf{r}_d of the dimension $M^2 \times 1$ can be computed via

$$\mathbf{r}_u = \mathbf{R}_u(\cdot), \quad (36)$$

$$\mathbf{r}_d = \mathbf{A} \mathbf{r}_u. \quad (37)$$

6. Construct the DCCM from \mathbf{r}_d , by sequentially grouping M elements of \mathbf{r}_d in columns to obtain an $M \times M$ matrix.

Once the DCCM for each user is computed, beam weights are calculated for the k_{th} user by fulfilling the below criteria

$$\frac{\mathbf{w}_k^H \mathbf{R}_{d,k} \mathbf{w}_k}{\sum_{n \neq k} \mathbf{w}_n^H \mathbf{R}_{d,k} \mathbf{w}_n + \sigma_k^2} \geq \gamma_k, \quad (38)$$

where σ_k and γ_k are the noise power and SINR for the k^{th} user, next, \mathbf{W} is normalized. Note \mathbf{w}_k in the above equation is given by the eigenvector corresponding to the maximum eigenvalue of the generalized eigenvalue problem

$$\mathbf{R}_{d,k} \mathbf{w}_k = \left(\sum_{n \neq k} \mathbf{R}_{d,k} + \sigma_k \right) \mathbf{w}_k. \quad (39)$$

4.6 Joint user grouping and beamforming

With increasing the number of users beamformed, the interference increases significantly, and the used techniques for beamforming, are not able to calculate weights that can make the users' streams orthogonal to each other.

As will be shown in the results section, each used technique can handle a number of users, where after that, leakage between users starts to appear, plus, interference and Bit-Error-Ratio (BER) grow. Therefore, in this section, the joint user grouping solution is proposed where the users will be placed in groups, and users in one group will be beamformed together. The groups are separated into different frequency-time resources, and the interference is canceled between the groups, due to the robustness of the LTE system. This will result in better performance in terms of BER and interference cancellation, however, the spectrum efficiency will be reduced, and that is the compromise that must be done here. The proposed grouping will be applied only to the AOA and the FC methods.

1. AOA Grouping

As the name suggests, the AOA method depends largely on the angle of arrival, and the method's performance decreases significantly if the dominant AOA of different users are not largely separated. Therefore, the criteria for placing users in different groups is the angular separation between users.

2. FC Grouping

As this method relies on downlink covariance matrix estimation, the criteria to separate users is the correlation between the downlink covariance matrices for two users. The metric of correlation between two covariance matrices is used from [44], and is given by

$$d(\mathbf{A}, \mathbf{B}) = \sqrt{\sum_{i=1}^n \ln^2 \lambda_i(\mathbf{A}, \mathbf{B})}, \quad (40)$$

where \mathbf{A}, \mathbf{B} are the covariance matrices that the metric is being calculated for, λ is the eigenvalue of the generalized eigenvector for \mathbf{A}, \mathbf{B} .

5 System model using MATLAB

The model is based on previous thesis work "Adaptive Beamforming for Next Generation Cellular System" [7]. However, the fading channel model previously used was replaced by the WINNER2 channel model. Plus, the new FDD beamforming techniques that were discussed in section 4.5 were added. LTE toolbox and the WINNER2 channel model toolbox were used in this model. The model basically simulates TDD or FDD basic LTE system as will be described in details later.

The structure of the GUI was not changed, only new features like options for TDD/FDD simulation, different WINNER2 scenario, additional beamforming algorithm for FDD were added. The MATLAB model of GUI is depicted in figure 16.

5.1 Initial parameters

In order to generate the channel, these parameters must be defined first:

- Number of BS antennas.
- Number of UE antennas (will be the same for all UEs).
- Bandwidth, this will affect the number of subcarriers used as shown in table 1.
- Uplink and downlink frequency used, this will be related to TDD or FDD system, if the uplink and downlink are using the same or different frequencies.
- Used scenario, this is one of the 13 scenarios supported by the WINNER2 channel model. However, in this thesis, only 2 scenarios mentioned in section 3.3.2 were focused on.
- Adding UEs, the distance of each UE from the base station can be chosen, then, the UE will be placed on the given distance but with random angle within the 120° sector area. Plus, the UE velocity can be chosen also.
- LOS or NLOS case.
- Noise, shadow fading and pathloss can be disabled or enabled separately.

After that, the "Generate Channel(s)" button can be pressed, and the model will generate the corresponding channel as the steps mentioned in section 3.3.1.

5.2 Uplink

After the channel has been generated, the following parameters can be defined to start the transmission process:

- The gain for the BS and UE antennas.

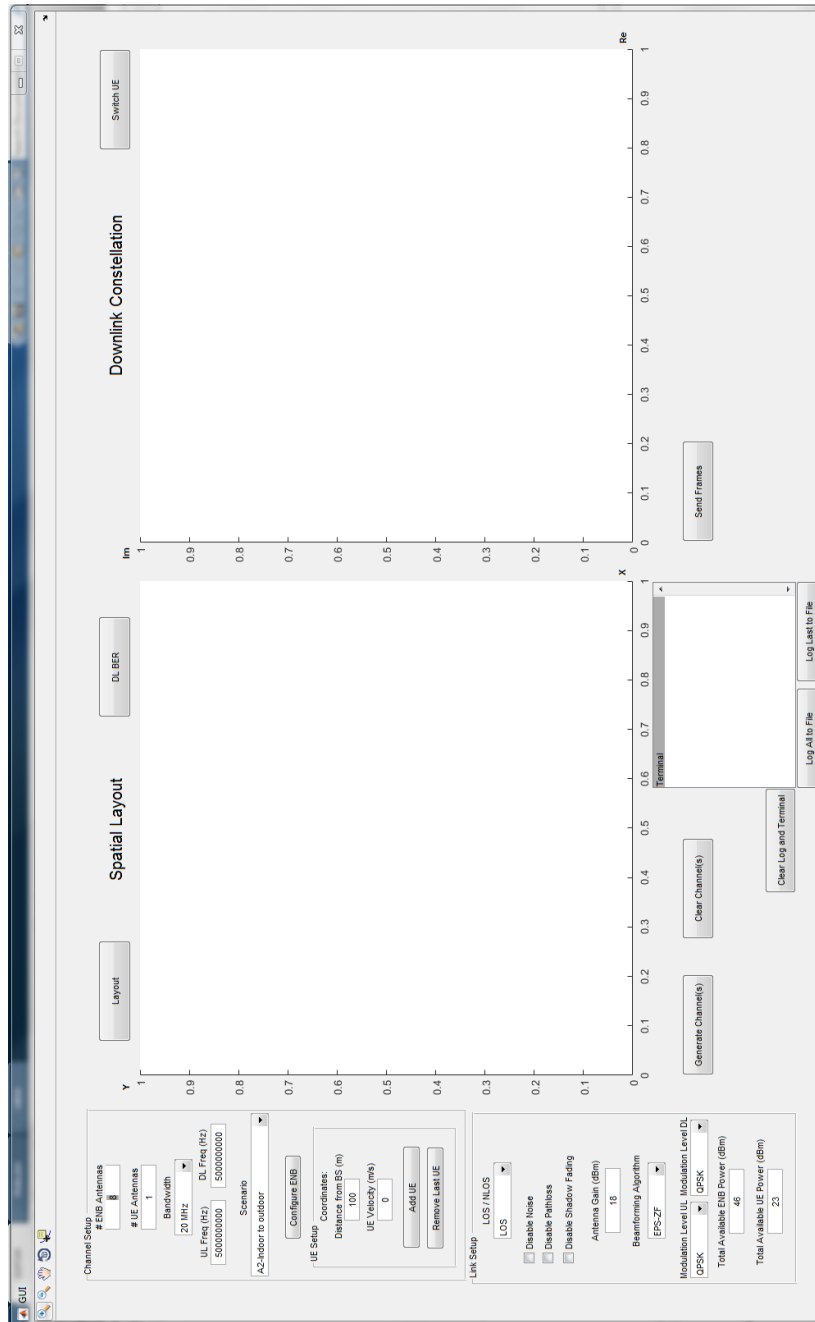


Figure 16: GUI of the MATLAB model.

- Beamforming algorithm used, and this based on the techniques that were studied in section 4, and it should be noted that for TDD systems the algorithms are:
 1. MRT.
 2. ZF.
 3. RZF.

While for FDD the algorithms are:

1. AOA MRT.
 2. AOA ZF.
 3. AOA RZF.
 4. Capon.
 5. FC.
 6. AOA Multibeamform.
 7. FC Multibeamform.
- Modulation schemes for uplink and downlink.
 - Power available at the BS and the UEs.

Once the mentioned parameters have been defined, the "send frames" button can be pressed. The uplink transmission process starts, where the UEs transmit one subframe to the BS.

The process begins with setting the UEs configurations. Next, for each user separately, one resource grid is generated, based on the configured bandwidth, then, random bits for UL-SCH are generated and saved for later BER calculation, and modulated to symbols based on the modulation scheme used. In addition, reference signals, as mentioned in section 2.5, will also be generated. Now, the indices for UL-SCH and DM-RS symbols in the resource grid are calculated, it is worth mentioning that in uplink, each UE has different indices from the others. After the indices are obtained, the DM-RS symbols are mapped to the resource grid, and the resultant grid is saved for later use by BS for channel estimation, then, the UL-SCH symbols can be mapped, and certainly unused indices that could be used by other users will be set to zero. The UE transmission process ends with SC-OFDMA modulation of the resource grid and frequency upconversion. Then, the Transmitted wave is ready to be sent after multiplying it with the available UE power defined earlier.

Later, the transmitted wave is passed through the channel between the BS antennas and the specified UE, and the antenna gain is multiplied with the signal, as mentioned earlier, the WINNER2 channel model gives the corresponding pathloss and shadowfading, only the noise is added by the model as mentioned in section 3.4. The mentioned process is repeated for all UEs.

After that transmitted waves are generated for all UEs and passed through their corresponding channels, the waves are summed up together as will be received by the BS antennas. Now, at the BS side, the received signal is frequency downconverted and SC-OFDMA demodulation is performed.

The mentioned process below is repeated for each UE individually. First, the BS estimates the channel for each UE from the saved reference grid, after that the channel estimation is obtained, the resource grid can be equalized as mentioned in section 2.4. Next, the APS and the dominant AOA is calculated for each user based on its equalized received signal, this part is only used in the FDD beamforming techniques. Now, the BS extracts the user UL-SCH symbols, as it knows the indices used by each user. Finally, the symbols are demodulated to bits and the BER for each user can be calculated based on the previously saved bits.

5.3 Downlink

After that one subframe has been received in uplink, the BS will transmit the next subframe, the process starts with creating the resource grid for each user, DM-RS symbols are generated and mapped to the resource grid, so that the resultant grid can be saved for later channel estimation by each UE. In addition, random bits for DL-SCH are generated and saved for later BER calculation and mapped to the grid. It should be noted, that in the downlink transmission, the DL-SCH and DM-RS indices for all UEs are the same because they will be beamformed, and this is the mentioned advantage for beamforming spectrum efficiency improvement, that it uses the same resource elements for all beamformed users. In this thesis scope, both DL-SCH and DM-RS symbols are beamformed. The Beamforming can be done based on the chosen beamforming algorithm, however, two cases must be differentiated.

1. TDD case: the model will loop through all the DM-RS and DL-SCH symbols indices, and for each symbol index it will get the corresponding estimated channel of the user, transpose it based on the channel reciprocity assumption, and then calculate the beamforming weights as mentioned in section 4.2, the same process is repeated for all UEs for that index. So, a weighting matrix is obtained and normalized in terms of power, and then multiplied with the corresponding users' symbols that will be sent on this index in the resource grid. The result is a number of symbols equal to the number of BS antennas that are decomposed of a weighted sum of users symbols for a certain index. This process will be repeated for all DM-RS and DL-SCH symbols. Therefore, the beamform weights are calculated for each resource element.
2. FDD case: Similar to the TDD case, however, the beamweights are calculated as mentioned in section 4.5 and this is done for all the resource grid, in other words, all UE's symbols will use the same weight and this is valid only because as mentioned earlier the used channel is frequency non-selective.

Now that the symbols have been weighted and each symbol resulted in multiple symbols equal to the number of BS antennas, they must be mapped to the antennas, and this is done by using the number of resource grids equal to the number of BS antennas. Next, OFDMA modulation occurs to transform the resource grids to transmitted wave, the transmission process ends with frequency upconversion and power scaling.

Later, the transmitted wave is received by each UE, by passing it through the UE corresponding channel, and if the beamforming calculation was correct, each UE will only receive its designated symbols, while other users symbols will be canceled when passed through the channel. Each UE frequency downconvert and demodulate its received signal to obtain a resource grid, the UE performs channel estimation from the already saved reference grid, now, the grid can be equalized as mentioned in section 2.4. Since each UE knows the indices of its DL-SCH, it can extract them from the grid, demodulates the symbols. Finally, BER calculation can be done.

6 Results

All the simulations are done for 3 MHz channel since it will result in a less frequency selective channel because all FDD models have the same beamforming weights for all the resource elements. Since all users are transmitting with the same power, so the distance between BS and all UEs are kept same. This assures that all UE will encounter almost same path loss.

A cell is divided into 3 sectors each with 120° coverage area. Thus, a BS serves only one sector and all UEs are distributed randomly along the circumference of third of a circle with a fixed radius. Noise is included in all simulation runs as per section 3.4. Until stated otherwise entire resource grid is assigned to each UE in the downlink. Further, all simulations are done for 1 layer, 1 UE antenna. The carrier frequency for TDD is 3 GHz, while for FDD is 3 GHz in uplink and 4 GHz in the downlink.

6.1 SINR and number of users

All the algorithms are compared with respect to probability of SINR less than 3 dB and number of users, 3 dB SINR is chosen because above 3 dB, the SINR shows reasonable BER around 5% . The SINR for each user is calculated by repeating the transmission process multiple times for the same channel. First, all symbols for the user whose SINR to be computed are set to zero, this gives interference power for that user. Then, symbols for the rest of the users are set to zero, this gives signal power for that user. Now noise is calculated as per section 3.4. Finally, SINR is computed as $SINR(dB) = SingalPower(dB) - InterferencePower(dB) - NoisePower(dB)$. The results are obtained by averaging 100 independent simulation runs each time with a different channel. Results are plotted for D1 (section 3.3.2) and B1 (section 3.3.2) scenario for both LOS and NOLS case in figures 17 18 19 20 respectively.

When comparing different FDD algorithms, The Capon beamformer outperforms all other for D1 LOS case because of the narrow angular spread in D1 LOS. In other cases, Capon has the worst performance, because of the wide angular spread. This is because the window size for Capon (figure 15) is 3 db, and when we have wide angular spread, this 3 dB window size might become wider enough to cover other users APS. So, while calculating beamweights, this will result in high interference.

In the LOS case AOA-ZF and AOA-RZF outperform TDD-MRT, but in NLOS case this is not true. Since in LOS case we probably have one dominant AOA so we can direct all the power towards that angle. But in NLOS there are no dominant AOA, so directing the beam towards only one angle will result in high loss of power. Mostly in NLOS case FC, AOA-ZF, and AOA-RZF have similar performance. It is obvious that TDD-ZF, TDD-RZF outperforms FDD, and for all of FDD algorithms, their performance decreases significantly for more than 3 users. This is because all FDD algorithms depend on APS of users for estimating beamweights, and as the number of users increases, the difference

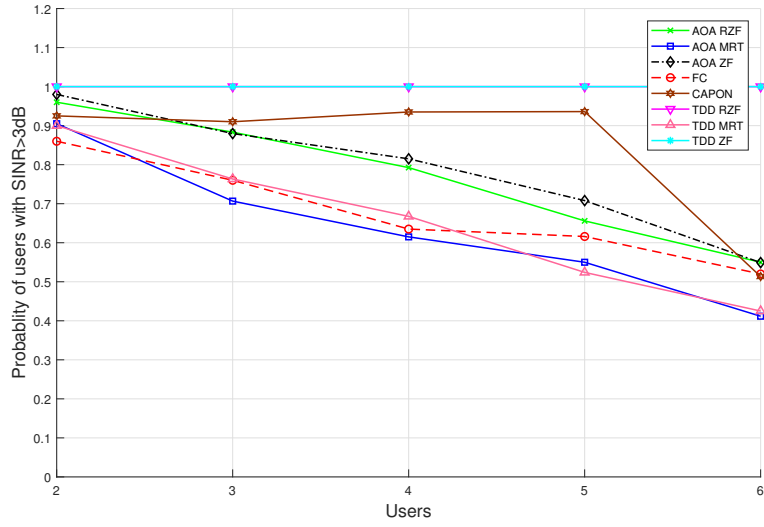


Figure 17: Probability of $\text{SINR} \geq 3$ dB vs number of users for D1 LOS scenario.

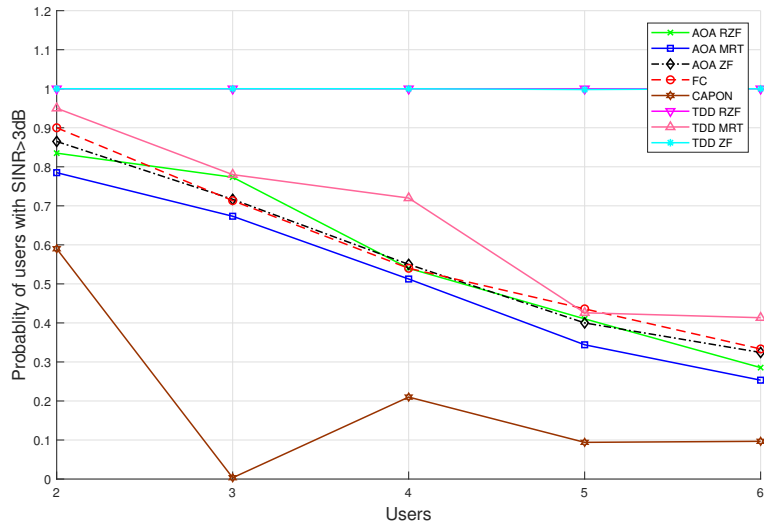


Figure 18: Probability of $\text{SINR} \geq 3$ dB vs number of users for D1 NLOS scenario.

between APS of users reduces.

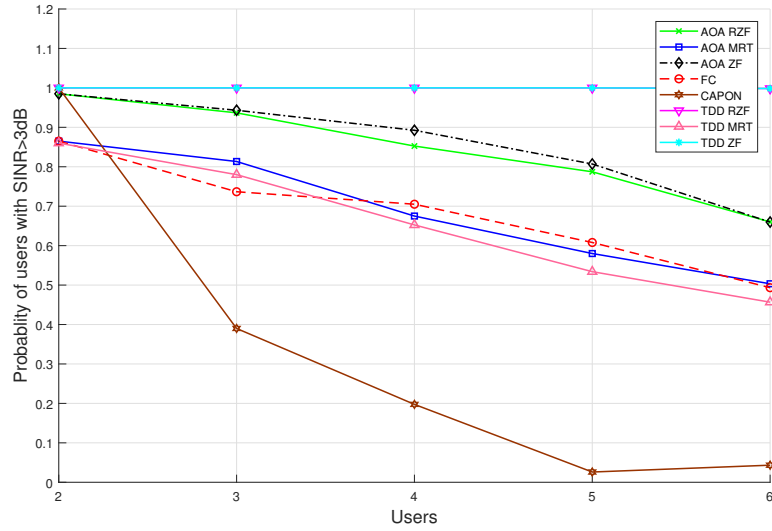


Figure 19: Probability of $\text{SINR} \geq 3$ dB vs number of users for B1 LOS scenario.

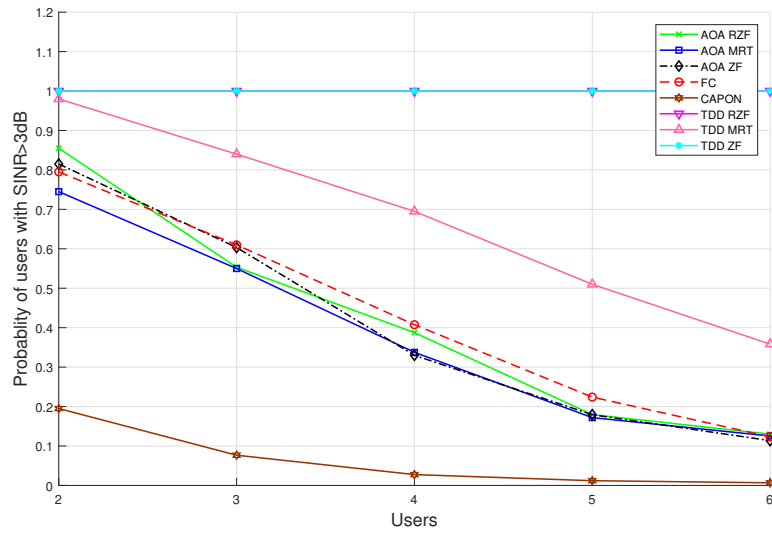


Figure 20: Probability of $\text{SINR} \geq 3$ dB vs number of users for B1 NLOS scenario.

6.2 BER and number of users

All algorithms are compared for average BER and number of users. The BER is computed by taking the average of 100 independent simulation runs each with a different channels.

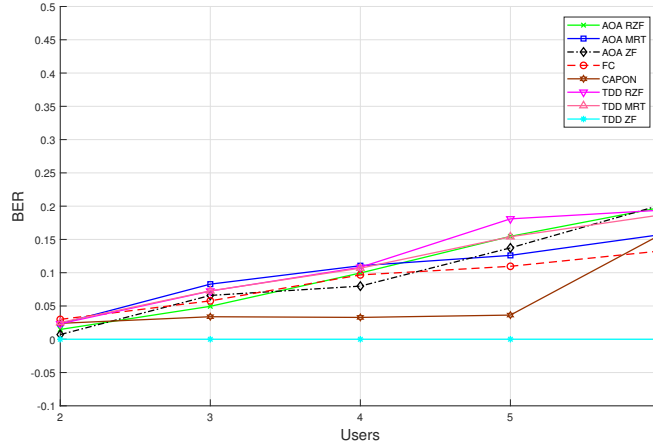


Figure 21: Average BER vs number of users for D1 LOS scenario.

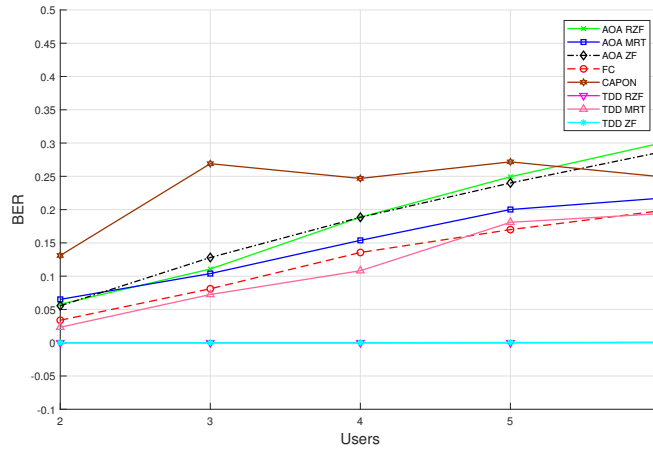


Figure 22: Average BER vs number of users for D1 NLOS scenario.

Since BER is related to the SINR received by the user, similar results to the previous simulation results are shown. The FDD algorithms have better BER in the D1 LOS scenario than B1 LOS, mainly because in rural areas the

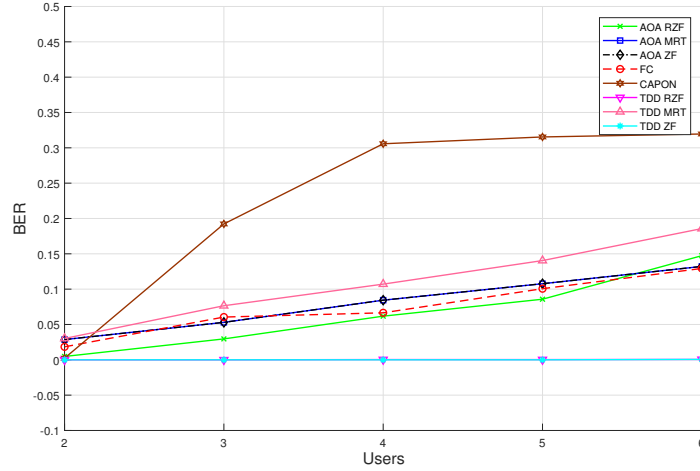


Figure 23: Average BER vs number of users for B1 LOS scenario.

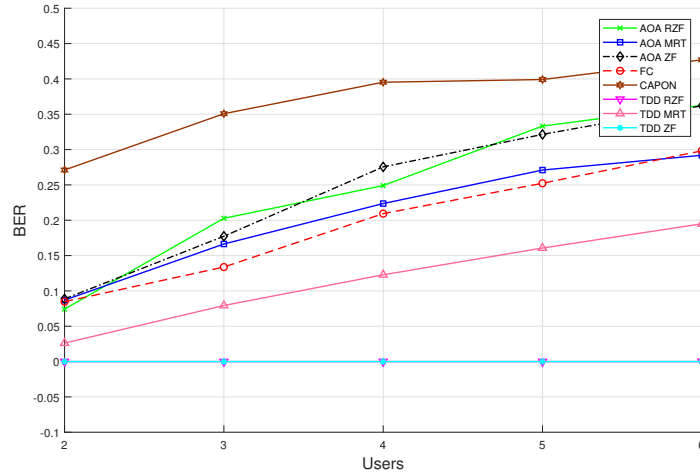


Figure 24: Average BER vs number of users for B1 NLOS scenario.

dominant AOA arrives with a higher power since it experiences fewer reflections. All the FDD algorithms degrade significantly, except for Capon in the D1 LOS case, for the reason mentioned earlier. It is also noticed that for the LOS case, the FDD algorithms outperforms TDD-MRT in BER. In here also, it is obvious TDD-ZF and TDD-RZF outperforms the FDD algorithms and show very robust performance with the increasing number of users.

As a conclusion for this section of simulation, the FDD beamforming al-

gorithms can be used for at most 3 users in D1 scenario and 2 users for B1 scenario for the simulation settings used above, and all the used algorithms depend largely on Angle of arrival, and better results are obtained for the LOS case. and most importantly, beamforming in TDD systems is far more efficient to use.

6.3 Performance with number of antennas

After finding that used FDD beamforming algorithms in B1 NLOS scenario cannot be used for more than 2 users when using 8 Tx antennas, The simulation below checks if the FDD beamforming problem is related to the number of antennas since the mentioned algorithms are highly dependent on AOA. Therefore, increasing number of antennas will result in better AOA estimation. The simulation is performed for 3 users, B1 NLOS case, where BS antennas vary from 4 to 12, the results are taken for 100 simulation runs.

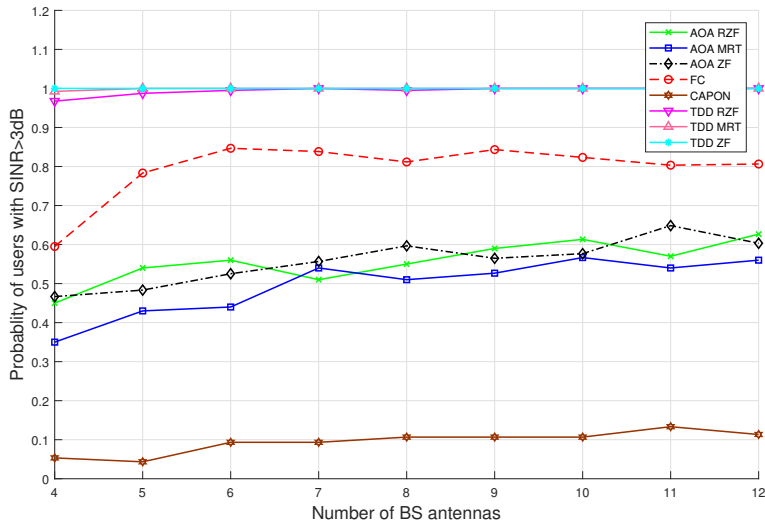


Figure 25: Probability of $\text{SINR} \geq 3$ dB vs number of BS antennas for B1 NLOS scenario.

It can be seen from figure 25 that the performance improves when increasing the number of antennas, due to the fact that increasing number of antennas will result in a narrower beam in downlink and thus, reduce the probability of interference. In addition, for FC better DCCM estimation is obtained.

6.4 Performance with Doppler shift

Since beamforming weights are calculated based on the uplink channel measurements, and then they will be applied in the subsequent downlink transmission. Therefore, it is required that the channel is correlated enough in time that the beamforming weights from the uplink channel measurements are valid. To study this, the performance of different algorithms has been analyzed with respect to Doppler spread.

The results in figure 26 show the variation of the probability of users with SINR greater than 3 dB with respect to Doppler frequency. Reason for choosing 3 dB SINR and method to calculate SINR is same as in section 6.1. Simulation is run for 2 UE each moving with a given velocity and B1 scenario (section 3.3.2) with a distance between BS and UE around 1000 m. Velocity is varied from 1 m/s to 18 m/s for each user this gives Doppler shift from 13 Hz to 240 Hz respectively. Simulation is stopped at 18 m/s because B1 scenario in WINNER2 is valid for UE velocity up to 19.44 m/s. Doppler shift for the corresponding velocity is calculated as per equation 3 and is computed for maximum Doppler. Results are obtained from 50 simulation runs.

From the results, we can see that all the methods are invariant for Doppler shift in given range. This is because most of the FDD methods depend on AOA which remains constant for a relatively long interval of time.

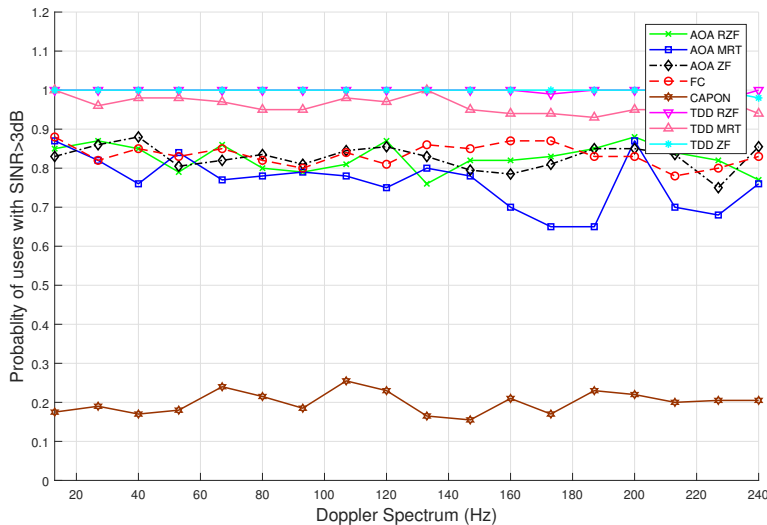


Figure 26: Probability of $\text{SINR} \geq 3$ dB vs Doppler shift for B1 NLOS scenario.

6.5 Computational complexity

Since the simulation is done in MATLAB, which runs over Windows operating system, comparison for computation complexity based on the runtime of code will not be a fair comparison. Since the computational time not only depends upon the frequency but also on the cache memory, how much program will be parallelized by MATLAB, RAM memory available and other parameters which are out of the scope of this thesis. Here we compare two algorithms mainly AOA and FC.

1. AOA Algorithm

For dominant AOA estimation MUSIC algorithm is used, as mentioned in sec 4.5.2. Computational complexity of MUSIC algorithm for ULA is given by $\mathcal{O}(M^2P + M^2N)$ [45]. Where M is the number of BS antennas, P is the number of MPC whose AOA is to be estimated and N is number of snapshots of signal needed for accurate AOA estimation. As in [45] only one snapshot of a signal is sufficient to estimate the AOA. Since AOA method uses only one dominant MPC of each user to estimate downlink impulse response, thus, the complexity of the AOA method reduces to $\mathcal{O}(2M^2)$. Also once the downlink impulse response is estimated, ZF beamforming is applied which needs matrix inversion, the computational complexity for matrix inversion is $\mathcal{O}(M^3)$ for an MXM matrix.

2. FC Algorithm

The FC matrix calculated in step 4 of section 4.5.3 is one time process, so, computational complexity for this will not be considered for comparison. Now, computer complexity DCCM from UCCM as in step 5 of section 4.5.3 is $\mathcal{O}(M^4)$ for uniform rectangular array and $\mathcal{O}(M^2)$ for ULA [13]. Now, to calculate weights for DCCM, SVD is required as in step 5 of 4.5.3 which is generally computationally intensive, of order $\mathcal{O}(M^3)$ for an MXM matrix. However, direct SVD calculation can be avoided as researchers have proposed various iterative approaches to calculate SVD, one example is [46].

6.6 Performance limitation

As mentioned in section 4.6, the performance is limited by AOA separation for the AOA method, and the correlation between the covariance matrices for the FC method. Therefore in this section, the threshold for separating users into different groups will be studied. The results in this section are obtained by 200 simulation runs for 6 users and 8 BS antennas for B1 NLOS case with an average distance of 1000 m from the BS station. for the figures in this section, the left y-axis represents the percentage of users having $\text{BER} \leq 5\%$, while the right y-axis represents, the percentage increase in capacity with respect to no beamforming done.

First, the AOA method is studied, as mentioned earlier, the threshold is the angle of separation between the dominant AOA's of users. Users are placed in

groups in such a way that all users within a group have an angular separation between their dominant AOA's larger or equal to the chosen threshold, this will result in better BER performance, as users that cannot separate their streams will not be beamformed. As shown in figure 27, the AOA method highly relies on the AOA separation, as with increasing the threshold (AOA separation), the BER performance improves, however the percentage increment in capacity reduces.

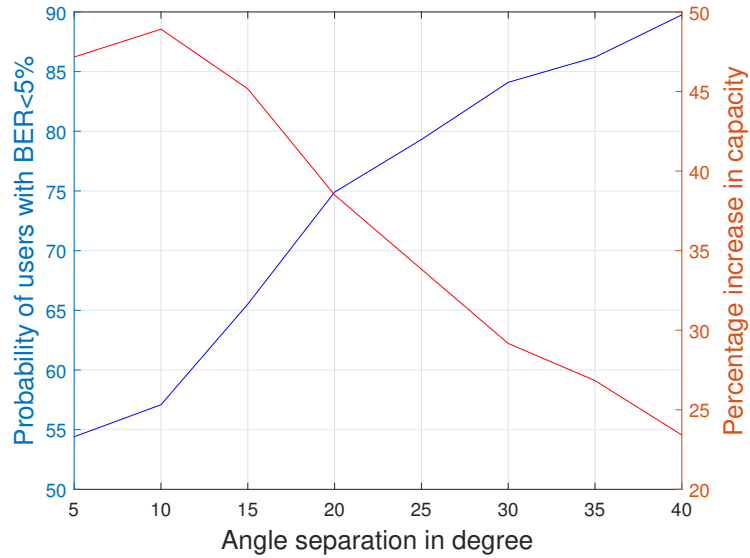


Figure 27: AOA-ZF group beamforming performance.

Secondly, the FC method is studied, the threshold here is relative to the best 2 least correlated users. for example, 0.1 threshold represents a maximum correlation between the covariance matrices of any two users in a group is smaller than 0.1. As shown in figure 28 Similar to AOA method, the FC highly relies on the correlation between users, this can be shown from the figure, when increasing the threshold, the BER performance improves, however, the percentage increment in capacity reduces.

When comparing the AOA and FC threshold study, the FC provides a better increment in capacity for same BER performance compared to AOA.

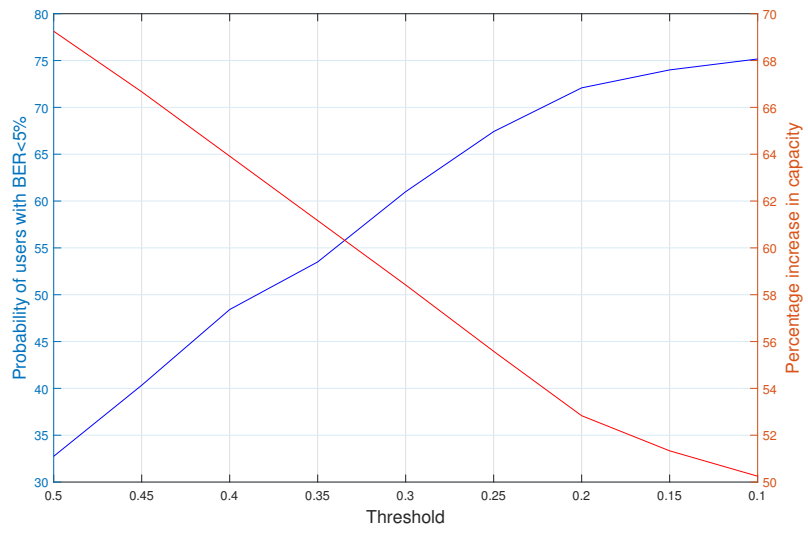


Figure 28: FC group beamforming performance.

7 Conclusions and future work

The thesis objective started as a simple question whether is it possible to do beamforming in FDD MIMO systems with partial downlink channel and if yes, how does the performance compare to TDD. Based on the obtained results, open loop FDD beamforming is possible using the mentioned techniques, but under very limiting conditions such as the number of users.

The Capon method is very sensitive for the width of the chosen window, so, the performance degrades significantly if the window size is not chosen accordingly, because it depends on the Angular spread which varies with different scenarios and users, as a consequence, choosing a wider window might result in high interference for other users. Meanwhile, the AOA and FC has shown more robust performance than Capon, nonetheless, AOA performance degraded more than FC when it comes to increasing number of users, due to the fact that when increasing number of users, the angular separation between users will decrease, which makes it harder to create orthogonal streams for users. Plus, results will improve if coding is used, as mentioned in this thesis work no coding has been used.

It can be observed from the results that the performance in term of SINR for the AOA, FC, and Capon methods improve with increasing number of the BS antennas, for the AOA method the increase in the number of the BS antennas will result in narrower downlink beam thus result in less interference. Meanwhile, for the FC and the Capon methods, better UCCM estimation is obtained. Also, it can be observed from the results that all the applied FDD methods are invariant with the Doppler spread in the simulated range of the Doppler spread. This is because AOA and UCCM remains relatively constant for long time interval with respect to the channel impulse response.

For computational complexity, AOA method has less complexity in our model, however, as mentioned in section 6.5 FC method complexity can be reduced and could become more efficient than AOA. However, it should be noted that in FC method, additional memory is needed to store the FC matrix.

While the performance of FDD beamforming techniques reduced significantly for more than 2 users. Still, for FC method, we can increase the spectral efficiency of the system by 50% if users are grouped with some criteria. On the other hand, overall improvement in spectral efficiency for AOA method was only 20% , when being compared to no beamforming case. However, beamforming in TDD is by far better than the studied FDD beamforming algorithms in all results discussed in this work.

Future work:

This thesis work only concentrated on evaluating beamforming weights based on AOA reciprocity. However, there are many more techniques in FDD beamforming in the literature, some are based on improving the techniques we used, and some on different approaches. A combination of open loop closed loop techniques could be studied to further improve the performance of the used techniques, as the feedback could contain information about the independent

fading which was neglected in the used techniques, this would yield better down-link channel estimation. Since the WINNER2 channel model supports system level simulation (multiple BSs), a more complex configuration can be studied and new parameters can be looked into like Inter-cell interference.

References

- [1] A. Paulraj, R. Nabar, and D. Gore, “Introduction to Space-Time Wireless Communications”. New York: Cambridge University Press, 2003.
- [2] A. Gupta, R. K. Jha, ”A survey of 5G network: Architecture and emerging technologies”, *IEEE Access*, vol. 3, pp. 1206-1232, 2015.
- [3] E. G. Larsson, O. Edfors, F. Tufvesson, T. L. Marzetta and B. Labs “Massive MIMO for Next Generation Wireless Systems”, *IEEE Communications Magazine*, Volume 52, Issue 2, February 2014.
- [4] X. Zhang, J. Tadrous, E. Everett, F. Xue, and A. Sabharwal, “Angle-of-arrival based beamforming for FDD massive MIMO” 49th Asilomar Conference on Signals, Systems and Computers , November 2015, pp. 704–708.
- [5] J. Nam, “Joint Spatial Division and Multiplexing: Realizing Massive MIMO Gains with Limited Channel State Information”, 46th Annual Conf. Information Sciences and Systems, 2012.
- [6] Andreas F. Molisch, “Wireless Communications”, Wiley Publishing, 2011.
- [7] S. Andersson, W. Tidelund, “Adaptive Beamforming for Next Generation Cellular System”, Masters Thesis Lund University, Sweden, September 2016.
- [8] E. Björnson, E. G. Larsson, and T. L. Marzetta, “Massive MIMO: Ten myths and one critical question” *IEEE Communications Magazine.*, vol. 54, no. 2, pp. 114–123, Feb. 2016.
- [9] G. Xu and H. Liu, “An effective transmission beamforming scheme for Frequency-Division-Duplex digital wireless communication systems,” *International Conference on Acoustics, Speech, and Signal Processing*, IEEE Press, vol. 3, pp. 1729-1732, May 1995.
- [10] K. Hugl, K. Kalliola, and J. Laurila, “Spatial reciprocity of uplink and downlink radio channels in fdd systems,” *COST 273 Technical Document TD (02)*, vol. 66, p. 7, 2002.
- [11] S. Moradi, R. Doostnejad, and P. G. Gulak, “Downlink beamforming for FDD systems with precoding and beam steering,” *Proc. IEEE Global Telecommun. Conf. (GLOBECOM)* , Houston, TX, USA, Dec. 2011, pp. 1–6.
- [12] K. Hugl, J. Laurila, and E. Bonek, “Downlink beamforming for frequency division duplex systems,” *IEEE Glob. Telecom. Conf. (GLOBECOM)*, vol. 4, 1999, pp. 2097–2101.
- [13] Y.-C. Liang, F.P.S. Chin, “Downlink channel covariance matrix (DCCM) estimation and its applications in wireless DS-CDMA systems,” *IEEE Journal on Selected Areas in Communications*, vol. 19, No. 2, pp. 222-232, Feb. 2001.

- [14] <http://www.3gpp.org/>.
- [15] S. Sesia , I. Toufik , M. Baker, “The UMTS long term evolution: from theory to practice,” Wiley Publishing, 2009.
- [16] Christopher Cox, “An introduction to LTE: LTE, LTE-Advanced, SAE and 4G mobile communications,” Wiley Publishing, 2012.
- [17] Erik Dahlman , Stefan Parkvall , Johan Skold, “4G: LTE/LTE-Advanced for mobile broadband,” Academic press, 2011.
- [18] G. Lindell, “An introduction to digital communications,” 2004. compendium.
- [19] Van de Beek, J.-J., O. Edfors, M. Sandell, S. K. Wilson, and P. O. Borjesson. “On channel estimation in OFDM systems.” vehicular technology conference, IEEE 45th, volume 2, IEEE, 1995.
- [20] U. Madhow, “Fundamentals of digital communication,” Cambridge university press, Cambridge, 2008.
- [21] Hampton, J. R. “Introduction to MIMO communications”. Cambridge: Cambridge university press.
- [22] Da-Shan Shiu, G. J. Foschini, M. J. Gans, and J. M. Kahn., “Fading correlation and its effect on the capacity of multielement antenna systems’,” IEEE Trans. Commun., 48(3):502–513, March 2000.
- [23] S. Wyne, A. Molisch, P. Almers, G. Eriksson, J. Karedal, and F. Tufveson, “Statistical evaluation of outdoor-to-indoor MIMO measurements at 5.2 GHz,” in IEEE VTC-Spring, May 2005.
- [24] A. Chockalingam, B. S. Rajan, ”Large MIMO systems”, Cambridge, U.K.:Cambridge Univ. press, 2013.
- [25] . A. F. Molisch, A. Kuchar, J. Laurila, K. Hugl, and R. Schmalenberger, “Geometry-based directional model for mobile radio channels principles and implementation,” European transactions on telecommunications, vol. 14, no. 4, pp. 351 359, July 2003.
- [26] X. Gao. ”Massive MIMO in real propagation environments”. doctoral thesis, Lund university 2016.
- [27] A. F. Molisch, H. Asplund, R. Heddergott, M. Steinbauer, and T. Zwick, “The COST259 directional channel model-part I: Overview and methodology,” IEEE transactions on wireless communications, vol. 5, no. 12, pp. 3421 3433, Dec. 2006.
- [28] H. Asplund, A. A. Glazunov, A. F. Molisch, K. I. Pedersen, and M. Steinbauer, “The COST 259 directional channel model-part II: Macrocells,” IEEE transactions on wireless communications, vol. 5, no. 12, pp. 3434 3450, Dec. 2006.

- [29] N. Czink and C. Oestges, "The COST 273 MIMO channel model: Three kinds of clusters," in Proc. IEEE International symposium on spread spectrum techniques and applications, Aug. 2008.
- [30] L. Liu, C. Oestges, J. Poutanen, K. Haneda, P. Vainikainen, F. Quitin, F. Tufvesson, and P. D. Doncker, "The COST 2100 MIMO channel model," IEEE wireless communications, vol. 19, no. 6, pp. 92-99, Dec. 2012.
- [31] IST-4-027756 WINNER II D1.1.2 WINNER II interim channel models. v1.0, September 2007.
- [32] "Spatial channel model for multiple input multiple output (MIMO) simulations". Technical report 3GPP TR 25.996 V6.1.0, September 2003.
- [33] T. S. Rappaport, "Wireless communications: principles and practice", 2nd edition, Prentice Hall, 2002.
- [34] T. K. Lo, "Maximum ratio transmission", IEEE Transaction communications, vol. 47, no. 10, pp. 1458-1461, Oct. 1999.
- [35] D. Nguyen, T. Le-Ngoc, "MMSE precoding for multiuser MISO downlink transmission with non-homogeneous user SNR conditions", EURASIP J. Adv. signal process., vol. 85, no. 1, pp. 1-12, Jun. 2014.
- [36] Bengtsson, M and Ottersten, Björn. "Optimal and suboptimal transmit beamforming". Handbook of antennas in wireless communications.
- [37] G.G. Raleigh, S.N. Diggavi, V.K. Jones and A. Paulraj, "A blind adaptive transmit antenna algorithm for wireless communication", in Proc. ICC, IEEE, 1995, vol. 3, 1494-1499.
- [38] W. M. G. Diab, and H. M. Elkamchouchi, "A novel approach for 2D DOA estimation using cross-shaped arrays," antennas and propagation society international symposium, IEEE Press, pp. 1-4, Ju12008.
- [39] H. Liu and J. M. Mendel, "Azimuth and elevation direction finding using arbitrary array geometries," IEEE trans signal processing, vol. 46, no. 7, pp. 2061-2065, Jul 1998.
- [40] R. O. Schmidt, "Multiple emitter location and signal parameter estimation," in Proc. RADC spectrum estimation workshop, Griffiss AFB, NY, 1979, pp. 243-258.
- [41] J. H. Winters, "Optimum combining in digital mobile radio with cochannel interference", IEEE J. Select. Areas commun., vol. SAC-2, no. 4, pp. 528-539, 1984.
- [42] J. Capon, "High-resolution frequency-wavenumber spectrum analysis", Proc. IEEE, vol. 57, no. 8, pp. 1408-1418, Aug 1969.

- [43] R. Lorenz and S. P. Boyd, “Robust minimum variance beamforming,” *IEEE transactions on signal processing*, vol. 53, pp. 1684–1696, May 2005.
- [44] W. Forstner, B. Moonen, . “A metric for covariance matrices” Report of the dpt of geodesy and geoinformatics, 1999, Stuttgart University, pp. 113–128.
- [45] C. Stöckle, J. Munir, A. Mezghani, J.A. Nossek “DoA estimation performance and computational complexity of subspace and compressed sensing-based methods” WSA, 2015.
- [46] B. Yang. “Projection approximation subspace tracking.” *IEEE Trans. on signal processing*, 43(1):95–107, 1995.



LUND
UNIVERSITY

Series of Master's theses
Department of Electrical and Information Technology
LU/LTH-EIT 2018-664
<http://www.eit.lth.se>